Strål
säkerhets
myndigheten
Swedish Radiation Safety Authority

Authors: Tero Manngård
Jan-Olof Stengård

Research

2014:19

Evaluation of the Halden IFA-650 loss-of-coolant accident experiments 5, 6 and 7

Report number: 2014:19 ISSN: 2000-0456
Available at www.stralsakerhetsmyndigheten.se

SSM perspective

Background

Loss of Coolant Accidents (LOCA) are among the most demanding accidents that can happen in a Light Water Reactor (LWR). The lack of cooling and the drop in pressure impose large stresses on the nuclear fuel which would increase the risk of fuel rod damage and the subsequent release of active material. But LOCA is also an accident that the nuclear power plant is designed to withstand with a limited release of radioactivity to the surroundings. Limitations shall be put upon the use of the nuclear fuel, that the reactor core constitutes of, such that the core can go through a LOCA without giving rise to an accelerating amount of damage, spread of active material within the power plant and its personnel nor spread of radioactivity to the environment.

Resent research has shown that nuclear fuel that has been irradiated to a high burnup can fail at lower temperatures than as prescribed by current design criteria. Ballooning and rupture of the cladding tube can occur at temperatures around 800 °C instead of the stipulated 1200 °C and the damage can result in a movement of the fissile material inside the cladding tube and release through the rupture.

The research is performed as tests in research reactors and institutes around the world, the Halden research reactor is one example. The tests need to be analyzed in order to understand the phenomena acting on the materials; i.e. how the cladding expands, in what way the fissile fuel pellets crack and move, and what makes the cladding to finally break. This understanding will hopefully make it possible to use the fuel to a higher burnup in a safe way.

Objectives

The objective for SSM in this project is to interpret the test and to implement the observed behavior of the nuclear fuel in analytical tools.

Results

The analytical tools, which are fuel rod computer codes, that Quantum Technologies AB use and develop, contain models of several of the phenomena that are acting on the nuclear fuel (cladding temperature, fission gas driven pressure, strain and stress in the cladding, rod rupture, etc.) and how the separate effects interact in the complex integrated manner. The codes are under constant development and need to be compared with actual tests. In this report simulations of three tests in Halden (IFA-650.5,6 and 7) are described.

Although it is difficult to model complex accident scenarios, the results obtained by Quantum Technologies AB show that it can be achieved. The codes and models can reasonably calculate cladding temperature, strain and diameter increase as a function of time, and finally estimate the position of cladding rupture.

Need for further research

In the future, more tests on nuclear fuel in LOCA conditions will be performed and to some extent code development will determine which aspects need to be further tested. The tests will form a base for the codes and model development around the world. When sufficiently many tests have been performed it will be possible to develop codes that with high confidence predict the behavior of the materials in the reactor core during a LOCA.

Project information

Contact person SSM: Jan In de Betou
Reference: SSM2012/510

Strål
säkerhets
myndigheten
Swedish Radiation Safety Authority

Authors: Tero Manngård[1] and Jan-Olof Stengård[2]
[1]Quantum Technologies AB, Uppsala, Sweden
[2] VTT Technical Research Centre of Finland

2014:19

Evaluation of the Halden IFA-650 loss-of-coolant accident experiments 5, 6 and 7

Date: March 2014
Report number: 2014:19 **ISSN:** 2000-0456
Available at www.stralsakerhetsmyndigheten.se

This report concerns a study which has been conducted for the Swedish Radiation Safety Authority, SSM. The conclusions and view-points presented in the report are those of the author/authors and do not necessarily coincide with those of the SSM.

Contents

Abstract

The Halden reactor fuel rod loss-of-coolant accident (LOCA) tests, IFA-650 series 5, 6 and 7, are evaluated using two versions of the computer code `FRAPTRAN-1.4`. The test sample IFA-650.5 was refabricated from a fuel rod irradiated in a pressurized water reactor (PWR) to a rod burnup of 83 MWd/kgU. The IFA-650.6 test sample was refabricated from a VVER rod (Russian type of PWR rod) irradiated in the Loviisa-1 reactor (Finland), whereas the IFA-650.7 sample was taken from a preirradiated boiling water reactor (BWR) rod. The rod burnups of the IFA-650.6 and IFA-650.7 test samples were about 56 and 44 MWd/kgU, respectively. The PWR rod and VVER rod both failed during the LOCA tests at temperatures below and around 800°C by fuel cladding burst. The BWR rod failed by cladding burst at 1100°C. The results of our computer calculations are compared with measured data for the following parameters: (i) Cladding temperature as a function of time; (ii) Fuel rod pressure as a function of time; (iii) Cladding diameter at rupture versus axial position of the rod; (iv) Peak cladding temperature at rupture; and (v) Maximum cladding oxide layer thickness induced by the LOCA transient. The agreement between calculations and measurements and between the two versions of the utilized code is fair. The report offers brief descriptions of the tests, the computer codes, the computations and a summary of the results.

Sammanfattning

I Halden reaktorn pågår experiment i den så kallade IFA-650 serien, där bränslestavar utsätts för laster simulerande de som kan uppkomma vid ett postulerat härdhaveri orsakad av kylmedelsförlust (LOCA, loss-of-coolant accident). Prov 5, 6, och 7 ur denna serie utvärderas här med två olika versioner av datorprogrammet `FRAPTRAN-1.4`. Experimentstaven för prov IFA-650.5 tillverkades av en bränslestav som förbestrålats i en tryckvattenreaktor (PWR) till en utbränning av 83 MWd/kgU. Provobjektet till IFA-650.6 tillverkades av en VVER stav (rysk typ av PWR stav) som bestrålats i den finska Loviisa-1 reaktorn, medan provobjektet till IFA-650.7 togs från en förbestrålad kokarvattenreaktorstav (BWR stav). Utbränningarna hos provobjekten som användes i IFA-650.6 och IFA-650.7 uppgick till ungefär 56 respektive 44 MWd/kgU. Både PWR staven och VVER staven havererade under LOCA proven vid kapslingstemperaturer omkring eller under 800°C, genom brott i kapslingen. BWR staven havererade genom kapslingsbrott vid 1100°C. Resultaten från våra datorberäkningar jämförs med mätdata för följande parametrar: (i) Kapslingstemperatur som funktion av tid; (ii) Bränslestavtryck som funktion av tid; (iii) Kapslingsdiameter vid brott längs staven; (iv) Maximal kapslingstemperatur vid brott; och (v) Maximal oxidtjocklek framkallad av LOCA transienten. Överensstämmelsen är någorlunda mellan beräkningar och mätningar samt mellan de två olika versionerna av beräkningsprogrammet. I rapporten ges beskrivningar av de olika proven, datorprogrammen, beräkningarna och en sammanfattning av resultaten.

1 Introduction

This report is the continuation of our previous report (Manngård, Massih, and Stengård 2012) on the evaluation of the Halden reactor IFA-650 tests to study fuel rod behaviour under LOCA conditions.

The IFA-650 series comprise both fresh fuel rods (tests 1 and 2) and high burnup rods which were irradiated in commercial pressurized water reactors or PWRs (tests 3, 4 and 5). Medium burnup fuel rods, irradiated in commercial power reactors, were used in the two subsequent tests, a Russian type PWR or VVER rod (test 6) and a boiling water reactor or BWR rod (test 7). The conditions for the tests were planned to satisfy the following objectives (Kekkonen 2007a; Kekkonen 2007b): (i) to maximize the ballooning of the cladding to enhance fuel pellet relocation and examine its consequence on cladding temperature and oxidation; (ii) to investigate the extent of "secondary transient hydriding" on the cladding inner side around the burst region. In addition to these two objectives, the intention with the BWR rod test (Jošek 2008) was to produce data on BWR fuel behaviour under LOCA and: (iii) to gain further understanding on the axial fuel relocation observed in earlier test (test 4). Fuel relocation occurs due to an opening of, or an increase in pellet-cladding gap and possible quivering of the fuel rod due to burst. Secondary transient hydriding refers to zirconium-steam reaction at the inner side of the cladding, upon cladding burst, which releases hydrogen gas, a portion of which is absorbed by the cladding, building zirconium hydride with brittling effect.

In the present work, we have used the `FRAPTRAN` computer code (Geelhood, Luscher, and Beyer 2011b) to evaluate three of the tests in the IFA-650 series, namely, tests 5, 6 and 7 (Kekkonen 2007a; Kekkonen 2007b; Jošek 2008). The results of our computations are compared with measured data for the following parameters: (i) Cladding temperature as a function of time during the transient; (ii) Fuel rod pressure as a function of time; (iii) Cladding diameter at rupture versus axial position of the rod; (iv) Peak cladding temperature at rupture; and (v) Maximum cladding oxide layer thickness induced by the LOCA transient. Two versions of `FRAPTRAN-1.4` were used in our evaluations for the sake of benchmarking; namely `FRAPTRAN-QT1.4c` (Jernkvist 2012) adapted in Quantum Technologies and `FRAPTRAN-GENFLO` developed by Technical Research Centre of Finland (VTT), which connects `FRAPTRAN-1.4` with the thermal-hydraulic program `GENFLO` (Miettinen and Hämäläinen 2002). Even in the `FRAPTRAN-QT1.4c` computations of the IFA-650 tests, we have used the thermal-hydraulic boundary conditions calculated by `FRAPTRAN-GENFLO`. That is, we have employed the `FRAPTRAN-GENFLO` calculated time variations of the coolant pressure, plenum gas temperature and cladding outer surface temperatures as prescribed boundary conditions in `FRAPTRAN-QT1.4c`.

The `FRAPTRAN-QT1.4b` code has previously been verified (Manngård, Jernkvist, and Massih 2011) against high temperature cladding burst data obtained from the German REBEKA series of LOCA experiments (Erbacher, Neitzel, and Wiehr 1990). The sole difference between the versions `QT1.4b` and `QT1.4c` of the `FRAPTRAN` program is that the latter version has been extended with material models for Zr1%Nb cladding needed in the present work (test 6). The `FRAPTRAN-QT1.4b` calculations of the IFA-650 tests 2, 3 and 4, reported in (Manngård, Massih, and Stengård 2012) and the `FRAPTRAN-QT1.4c` calculations of the tests 5 and 7 in this report use the average (best-estimate) stress-base failure criterion by Rosinger (1984). For test 6, we apply the stress-base failure criterion (Zr1%Nb cladding) proposed by Van Uffelen and coworkers (2008). However, in our former set of calculations (tests 2, 3 and 4), we used total oxygen concentration value (sum of oxygen content in metal and oxide layer) in the burst correlation, whereas in the actual calculations (tests 5, 6 and 7) we instead apply the oxygen content in the metal to obtain the burst stress. The `FRAPTRAN-GENFLO` calculations use a strain-base cladding failure criterion available in the `FRAPTRAN-1.4` program (Geelhood, Luscher, and Beyer 2011b).

The report is organized as follows. Section 2 provides brief descriptions of the Halden IFA-650 tests considered in our evaluation. Here, we also include fuel rod design data, used as input to the codes, and a summary of the main results of the experiments. The versions of the employed computer codes are briefly described in section 3. The fuel rod calculations of the tests are presented in section 4, in which also the results of the calculations are compared with measured values. Input options to the codes are specified in Appendix A. Finally in section 5, we end the report by making some concluding remarks.

2 Halden IFA-650 experiments

The Halden IFA-650 series of tests refer to fuel rod experiments performed in the Halden boiling heavy-water reactor (HBWR) under simulated loss-of-coolant accident (LOCA) conditions. The test fuel rods used in experiments 5, 6 and 7, which are analyzed in this report, were refabricated from full-length rods pre-irradiated in different commercial nuclear power reactors. The test rods were filled with a gas mixture consisting of 95 vol.% (or 90 vol.%) argon and 5 vol.% (or 10 vol.%) helium to a pre-defined pressure at room temperature. Argon was selected to mimic the fission product gases, while a small amount of helium was needed to leak test the rod. The rod plenum volume (free gas volume) was made sufficiently large in order to maintain stable pressure conditions until cladding burst. The data for these test rods are summarized in table 1.

A schematic drawing of the IFA-650 test rig is shown in figure 1. The test rod is placed in the center of the rig and surrounded by an electrical heater inside the flask. The heater is part of a flow separator, which separates the space into a central channel adjacent the fuel rod and an outer annulus. The heater was used to simulate the isothermal boundary conditions, i.e. the heat dissipated from the nearby fuel rods during a LOCA. Cladding temperature is affected by both the fuel rod and the heater power. The rod power is controlled by varying the reactor power. The inner/outer diameters of the heater and pressure flask are 20/26.2 mm and 34/40 mm, respectively. The IFA-650 test rig instrumentation for the actual tests consisted of 3 cladding surface thermocouples, a fuel rod elongation detector, a fuel rod pressure transducer, two fast response cobalt neutron detectors and three vanadium neutron detectors, three heater thermocouples and coolant thermocouples at the inlet and the outlet of the rig. Certain thermocouples (TC) and their axial locations are summarized in table 2. The fuel pressure transducer (PF) is connected to the top part of the test fuel rod. The temperature of the heater is measured by three embedded thermocouples located axially at the bottom, mid and top levels of the fuel stack. The bottom and top level heater TCs are located approximately at the same axial elevations as the cladding thermocouples.

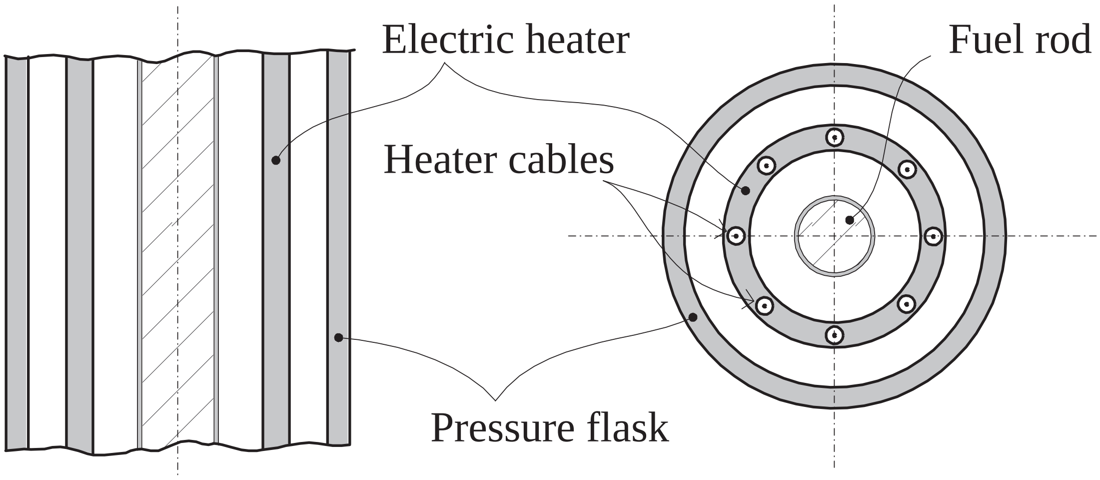

Figure 1: Schematic drawing of the IFA-650 test rig cross sections.

For experiment 5 and 6, a particle filter was installed in the outlet flow pipe (line) of the rig to prevent possible transport of fuel fragments and the associated spread of activity outside the rig after rod failure. More precisely, the filter in the rig was located roughly at the same axial level as the pressure transducer. No such filter was used in the earlier tests, 2, 3 and 4. Since the time for completing the blowdown in these two filter-equipped tests (5 and 6) were significantly longer than that in the preceding tests (2, 3 and 4), the filters may have reduced the coolant flow during the blowdown. Experiment 7 was performed without particle filter.

General description of test procedure:
In brief, the IFA-650 test procedure can be described as follows. Prior to the LOCA test the reactor power is tuned so that the predefined power level in the fuel rod is obtained. The heater is then switched on to its predefined constant power value. At this preparatory phase the reactor is operating under forced circulation (using an outer flow loop). After reaching the desired fuel power, the test rig is disconnected from the outer loop and the temperatures are left to stabilize under natural circulation for a few minutes before initiation of the LOCA transient (blowdown). The magnitude of the heat generation rates in the heater and fuel rod are selected with the aim to reach a desired (target) peak cladding temperature during the test.

The blowdown is initiated by opening the valves to the dump tank, whereby the rig is rapidly emptied of water (coolant). During the blowdown the coolant pressure falls quickly to a value close to that of the counterpressure in the dump tank. The coolant pressure (p_c) transient resulting from the blowdown operation is illustrated in figure 2. The associated responses of cladding temperature (T, dashed line) and rod internal gas pressure (p_g) are also depicted in the figure. The cladding temperature starts to rise quickly due to inadequate cooling of the rod. In addition, the linear heat rates for fuel rod (Q_f) and heater (Q_h) are schematically shown by the dash-dot lines in figure 2. Upon fuel rod failure (cladding burst) the rod pressure drops to the pressure of the surrounding coolant. Typically, as shown in figure 2, the heater is switched off shortly before test termination (reactor scram).

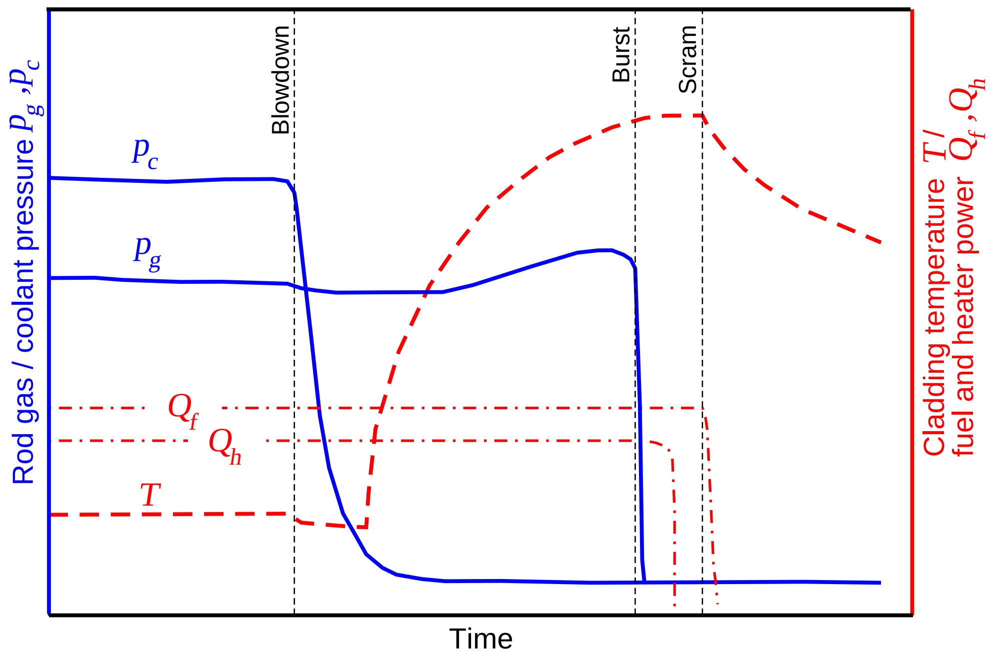

Figure 2: Schematic description of typical time responses of some selected parameters during a Halden IFA-650 LOCA experiment. The LOCA transient (test) is initiated by the blowdown and terminated by reactor scram.

2.1 IFA-650.5

In the fifth experiment, IFA-650.5 (Kekkonen 2007a; Oberländer, Espeland, and Jenssen 2008), an irradiated PWR UO_2 fuel rod with Zircaloy-4 base duplex (double layer) cladding (16×16 fuel assembly) with outer diameter and wall thickness of 10.735 mm and 0.721 mm, respectively, was tested. The outer cladding layer with a thickness 0.15 mm had a reduced tin content relative to the base material (0.84 wt.% versus 1.48 wt.%). The IFA-650.5 test rod was re-fabricated from a segment (between spacer grid 5 and 6) of the same full-length father rod that also provided the test sample for IFA-650.3. The segment for IFA-650.5 had an average burnup of 83 MWd/kgU. The active length of the re-fabricated test fuel rod was 480 mm. The test rod was filled with a gas mixture consisting of 90 vol.% argon and 10 vol.% helium to a pressure of 4 MPa at room temperature (Kekkonen 2007a). The base irradiation of the full-length rod comprised 6 reactor cycles corresponding to 1994 effective full power days (EFPD). The average linear power densities (for the segment) during the cycles were 37.5, 28.0, 22.0, 20.0, 18.0 and 18.0 kW/m, respectively. The data for the rod used in the IFA-650.5 experiment are summarized in table 1. The IFA-650.5 test rig design and instrumentation are described in (Kekkonen 2007a).

Prior to the LOCA test the heater power was turned on to a preset value of 1.7 kW/m. The heater power was kept constant at the preset level but was increased to $\approx$ 2.0 kW/m at later stage of the heat-up phase. The heater was switched off shortly before reactor scram (test termination). The fuel rod was kept at an average constant nuclear power of about 2.5

Table 1: IFA-650 test rod data. Numerical values are those of the as-fabricated ones except burnup, cladding outer oxide layer thickness and cladding hydrogen content.

Test number		5	6	7
PELLET:				
Material		UO_2	UO_2	UO_2
Diameter	mm	9.132*	7.55	8.19
Centre hole diameter	mm	-	1.484	-
Length	mm	11	10	10
Dishing		both ends	No	Yes
Dish depth	mm	0.28	-	...
Land width	mm	1.2	-	...
Density (UO_2)	% of TD	94.8	97.1	96
U-235 enrichment in UO_2	wt.%	3.5*	3.6	4.46
CLADDING:				
Material		DX ELS0.8b‡	E110 (Zr1%Nb)	Zircaloy-2†
State		SRA♭	...	...
Outer diameter	mm	10.735*	9.13	9.62
Wall thickness	mm	0.721*	0.679	0.63
Outer oxide layer thickness (mean/max)	μm	65/80	≈ 5	4.4 (mean)
Hydrogen content	ppm	650	≈ 100	44
FUEL ROD:				
Burnup	MWd/kgU	83.4	55.5	44.3
Active length	mm	480	480	480
Total length of test rod	mm	1040	985	985
Radial pellet-clad gap	mm	0.0805*	0.1115	0.085
Plenum volume	cm^3	15	16-18	17-18
Fill gas		90%Ar+10%He	95%Ar+5%He	95%Ar+5%He
Fill pressure	MPa	4.0	3.0	0.6
Fabrication temperature	°C	25	25	25

* Actual value instead of nominal (unirradiated condition). ‡ Zircaloy-4 cladding with 150 μm thick outer layer of Zr alloy with reduced tin content (0.8 wt.% Sn) relative to the base material. (DX=Duplex, i.e. dual-layer material, ELS=Extra Low Sn) † Zircaloy-2 cladding with 70 μm thick inner layer of Zr alloy. ♭ SRA = stress relief anneal.

kW/m. The axial rod power profile was symmetric and slightly peaked in the middle (axial peak to average power ratio was ≈ 1.05; see figure 3). The LOCA test, initiated by opening the valves to the blowdown tank, emptied the rig of water in about one minute. During the blowdown phase the coolant pressure in the loop decreased from ≈ 7 MPa to ≈ 0.4 MPa. In the subsequent heat-up phase, the cladding temperature increased quickly. The peak cladding temperature (PCT) aimed at the test was 1100°C, whereas the PCT measured reached 1042°C (according to TCC1 recording). Cladding failure occurred ≈ 178 s after the blowdown at ≈ 750°C and was indicated by a marked drop in pressure signal followed by a slower decrease in pressure. The elongation detector signal also indicated by a subtle response at the instant of burst. After some delay (≈ 12 s) upon burst the gamma ray monitor on the blowdown line to the dump tank also confirmed the cladding failure. The

Table 2: Axial positions (in mm) of thermocouples used in the IFA-650 test rigs. The axial positions are relative to the fuel stack bottom end.

Test number	5, 6, 7
Thermocouples:	
cladding	100 (TCC1)
	400 (TCC2)
	400 (TCC3)
coolant/channel	...
plenum gas	...

average cladding temperature increase rate during the heat-up phase (prior to the burst) was 5.0-5.5°Cs^{-1}. Halden experimenters cooled the test rod by spraying (with water) after the cladding burst. The test was terminated by a reactor scram. The time from cladding burst to reactor scram was about 5 minutes.

After LOCA testing in Halden the rod was brought to the hot cell laboratory in Kjeller (Norway) for post irradiation examination (PIE). Visual examination of the rod revealed that the cladding had failed by a narrow $\approx$ 10 mm long axial crack located $\approx$ 20 mm below the lower cladding thermocouple (TCC1) position (Oberländer, Espeland, and Jenssen 2008). The term "narrow" means here that the crack had no visible opening (or clearance) between its fracture surfaces. The test results are summarized in table 3.

2.2 IFA-650.6

Test six, IFA-650.6 (Kekkonen 2007b), involved a fuel rod segment refabricated from a standard full-length VVER UO_2 fuel rod, which had been pre-irradiated in the Finnish Loviisa-1 reactor (VVER-440) for four cycles during the years 1998 to 2002. The average linear power densities during the cycles for this particular rod segment were around 20.0, 20.0, 17.5 and 11.5 kW/m, respectively (Pihlatie 2005). The fuel rod was equipped with E110 (Zr1%Nb) cladding with outer diameter and wall thickness of 9.13 mm and 0.679 mm. The active length of the refabricated test fuel rod was 480 mm. The data for the rod used in the IFA-650.6 experiment are summarized in table 1. The IFA-650.6 test rig design and instrumentation are described in (Kekkonen 2007b).

In the end of the preparatory phase (under forced circulation) of the test the fuel rod linear heat generation rate (LHGR) was reduced from the steady state power level of 8.0 kW/m to 1.2 kW/m by decreasing the reactor power. Taking into account the excess decay heat, the fuel linear heat rate was close to 1.3 kW/m. After reaching the desired rod power level the electrical heater was switched on. The predefined heater power for this test was set to 1.35 kW/m. The heater power was kept constant at 1.35 kW/m but was increased to 1.7 kW/m at a later stage of the heat-up phase. The heater was switched off shortly before reactor scram (test termination). The axial rod power profile was symmetric and slightly peaked in the middle (axial peak to average power ratio was $\approx$ 1.08; see figure 3). Next, the rig was disconnected from the outer loop letting the temperature in the rig to stabilize under natural circulation (self convection) flow during a few minutes before initiating the blowdown. At blowdown, the valves to the dump tank was opened and the rig was practically emptied of

Table 3: Summary of measured results from the considered IFA-650 tests.

Test number	5	6	7
Time to rupture after start of blowdown, s	178	525	247
Axial location[a] of rupture, mm	70-80	90-100	110-122[e]
Axial length of rupture (crack), mm	10	10	12
Max. lateral width of crack opening, mm	...	...	1-2
Av. rod pressure from blowdown to rupture, MPa	7.0[b]	6.3[bc]	1.04[b]
Rod pressure at rupture, MPa	7.2[b]	6.4[bc]	1.05[b]
Cladding diameter increase[d] close to rupture area, %	12	...	20-22
Max. cladding diameter increase[d] in rupture area, %	17[f]	36	22
Cladding-heater mechanical interference at rupture (Yes/No)	...	...	...
Cladding temperature at start of heat-up, °C	210	210	200
Cladding temperature at rupture, °C	750	830	1100
Av. cladding temperature increase rate during heat-up until rupture, °Cs^{-1}	5.0-5.5	1.7-1.9	9.0
Typical cladding azimuthal temperature variation during heat-up until rupture, °C	...	...	...
Max. measured cladding temperature:			
upper thermocouple position, °C	1002	769	1086
lower thermocouple position, °C	1042	832	1239
Cladding outer surface oxide layer, μm (increase under LOCA)	11	2	30

[a] From bottom end of fuel stack. [b] To obtain the differential pressure across the cladding wall, the rod pressure value shall be subtracted by the coolant channel pressure ($\approx$ 0.4 MPa) after blowdown. [c] The level of absolute rod pressure could not be defined precisely in the IFA-650.6 test (Kekkonen 2007b). [d] Estimated from measured diameter increase ΔD with respect to initial cladding outer diameter D_0 by $\Delta D/D_0 \times 100\%$. [e] Multiple axial cracks around primary rupture location (TC position). [f] Value obtained by visual inspection. The diameter increase by neutron radiography is 32% (Oberländer, Espeland, and Jenssen 2008).

water in less than a minute. During the blowdown the pressure in the coolant channel fell from around 4-5 MPa down to the rig pressure ($\approx$ 0.4-0.5 MPa).

During the heat-up phase, following the blowdown, the cladding was subjected to a temperature rise from 210 to 800°C in about 300 seconds (5 minutes). Halden experimenters cooled the test rod by spraying (small spray pulses with water) at 800°C (TCC1 signal). During the next 100 s the maximum measured cladding temperature rose (under spray cooling) by about 30°C before rod failure occurred. The target peak cladding temperature of 850°C was almost (832°C) reached in the test. More precisely, cladding failure occurred $\approx$ 525 s after the blowdown at $\approx$ 830°C. The time to cladding rupture was primarily detected by a rapid drop in the rod pressure signal (PF) and a small but distinct drop in the lower cladding thermocouple signal (TCC1). The average cladding heating rate up to the instant of rupture was around 1.7-1.9°Cs^{-1}. The test was terminated by a reactor scram. It should be noted that the absolute rod pressure level in the pressure measurement could not be defined precisely for the test (Kekkonen 2007b). However, retrieving rod pressure at burst from the PF recording reported from the test, we obtain a value of $\approx$ 6.4 MPa.

Oberländer and Jenssen (2011a) has later reported that the overpressure at burst was ≈ 5.2 MPa, however, the basis for this value is unclear. Also, the definition of the quantity referred to as overpressure is lacking in (Oberländer and Jenssen 2011a). However, assuming that "overpressure" here is equivalent with differential pressure across cladding wall, then rod pressure at burst would be ≈ 5.6 MPa (5.2+0.4 MPa, where 0.4 MPa is the rig pressure after the blowdown).

After LOCA testing in Halden, the rod was subjected to a PIE program at the Kjeller hot cell laboratory. The PIE revealed that the rod had failed by a small (≈ 10 mm long) crack close to the lower thermocouple position. A summary results from the test are given in table 3.

2.3 IFA-650.7

In test seven, IFA-650.7 (Jošek 2008; Oberländer and Jenssen 2011b), an irradiated BWR UO_2 fuel rod with Zircaloy-2 cladding with outer diameter and wall thickness of 9.62 mm and 0.63 mm, respectively, was tested. The cladding was equipped with a 70 μm thick inner layer (liner) of Zr alloy. The test rod was manufactured from a full-length rod pre-irradiated in the Swiss KKL reactor to a rod burnup of 44 MWd/kgU. The base irradiation of the full-length rod comprised 3 reactor cycles. The active length of the test fuel rod was 480 mm. The data for the rod used in the IFA-650.7 experiment are summarized in table 1. The IFA-650.7 test rig design and instrumentation are described in (Jošek 2008). The heater power was kept constant at ≈ 2.0 kW/m through most of the test with a temporary reduction to ≈ 1.5 kW/m. The fuel rod was kept at an average constant nuclear power of about 3.4 kW/m. The axial rod power profile was symmetric and slightly peaked in the middle (axial peak to average power ratio was ≈ 1.05; see figure 3).

The blowdown, initiated by opening the valves to the blowdown tank, emptied the rig of water in about one minute. During the blowdown phase the coolant pressure in the loop dropped from about 7.0 MPa to 0.4 MPa. In response to the inadequate cooling of cladding from completed blowdown, the heat-up phase started, during which the cladding was subjected to a fast temperature rise from ≈ 200 to 1100°C in about 200 seconds. The target peak cladding temperature of 1150°C for the test was reached 254 s after blowdown initation. Halden experimenters started cooling the test rod by spraying (with short pulses of water) at cladding temperature of 870°C. The test was terminated by a reactor scram 311 s after start of blowdown. The heater was switched off shortly after the scram. Cladding burst occurred 247 s after the start of the blowdown at a cladding temperature of around 1100°C indicated by a sharp drop in the rod pressure signal (PF). After a delay of ≈ 10 s upon burst (determined by PF signal) the gamma ray monitor on the blowdown line to the dump tank also responded to the cladding failure. The average cladding temperature increase rate during the heat-up phase (prior to burst) was $\approx 9°\mathrm{Cs}^{-1}$.

After LOCA testing in Halden the rod was subjected to various examinations at the hot cells in Kjeller. Visual inspection revealed that the rod failed in the area of the lower thermocouple. Furthermore, the rupture region showed multiple cracks oriented in axial direction. The primary failure (a lens-shaped crack) is 12 mm long with a 1-2 mm wide burst opening in its centre. The test results are summarized in table 3.

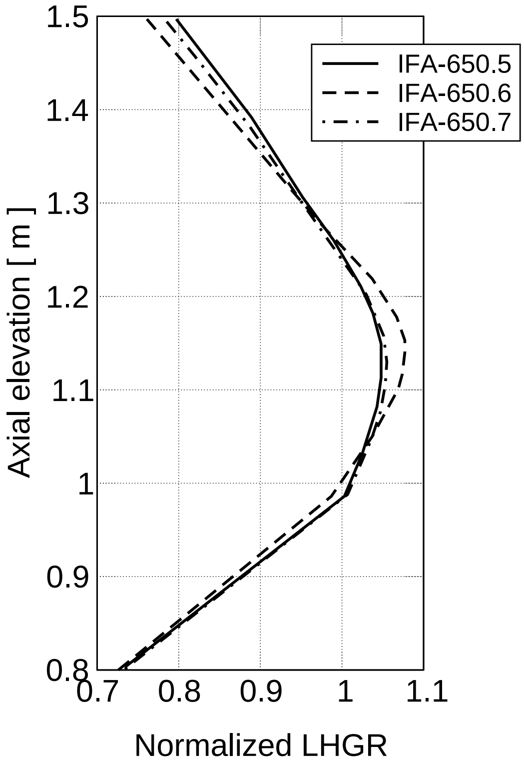

Figure 3: Axial power distributions produced by nuclear fission in the IFA-650.5/6/7 test fuel rods in the Halden reactor. Axial elevation versus normalized linear heat generation rate, adapted from (Kekkonen 2007a; Kekkonen 2007b; Jošek 2008). The lower end of the fuel stack is located at the axial elevation of 0.9 m.

3 Computer codes

For the analysis of the Halden experiments considered in this report, we have utilized two variants of the computer program `FRAPTRAN-1.4`, namely, (i) `FRAPTRAN-QT1.4c` comprising an implementation of the model presented in (Manngård and Massih 2011) in `FRAPTRAN-1.4`, and (ii) `FRAPTRAN-GENFLO` developed by Technical Research Centre of Finland (VTT), which connects `FRAPTRAN-1.4` with the thermal-hydraulic program `GENFLO` (Miettinen and Hämäläinen 2002). Brief descriptions of these codes and appropriate references to their detailed accounts are given below.

The code `FRAPTRAN` (Fuel Rod Analysis Program Transient) simulates the light water reactor fuel thermal-mechanical behaviour when power and/or the coolant boundary conditions are rapidly changing (Geelhood, Luscher, and Beyer 2011b). More specifically, the code computes fuel rod attributes, such as fuel and cladding temperatures, cladding elastic and plastic strains, cladding stresses, fuel rod internal gas pressure, etc. as a function of irradiation time. `FRAPTRAN` affords a best-estimate code for analysis of fuel response to postulated accidents such as LOCA and interpreting experiments simulating such accidents. The `FRAPTRAN-1.4` code assessment, that is, comparison between code computations and data from selected integral irradiation experiments and post-irradiation examination programs is documented by Geelhood et al. (2011c). The standard models and modelling options available in FRAPTRAN-1.4 are described in (Geelhood, Luscher, and Beyer 2011b). The models implemented in the version 1.4 of FRAPTRAN can be used with the finite element based solution module of the code developed by Knuutila (2006). Fuel rod variables that are slowly varying with time (burnup), such as fuel densification and swelling, and cladding irradiation creep and growth, are not calculated by FRAPTRAN. But, the state of the fuel rod at the time of a transient, which depends on those variables can be read from a file generated by the companion steady-state code FRAPCON-3.4 (Geelhood, Luscher, and Beyer 2011a).

The FRAPTRAN-QT1.4c computational method is similar to that described in (Manngård and Massih 2011) with some extensions, modifications and adaption to an integral fuel rod modelling code (Jernkvist 2012). The main quantities calculated by the method are (i) oxygen parameters, which can be either the oxygen concentration picked up by the cladding during the oxidation process, the oxide layer thickness, or the oxygen concentration in the cladding metal layer; (ii) the volume fractions of the α-Zr and β-Zr during the phase transformation; (iii) the cladding hoop strain due to creep; and (iv) a cladding burst stress criterion. All these quantities are coupled through a set of kinetic (differential) equations and the burst criterion, which are solved numerically. The FRAPTRAN-QT1.4c models are used with the aforementioned finite element solver of FRAPTRAN-1.4.

The FRAPTRAN-GENFLO code is a coupled reactor core thermal-hydraulic and fuel rod analysis package. GENFLO simulates the thermal-hydraulic behaviour of a fluid channel (surrounding a fuel rod) during LOCA conditions (Miettinen and Hämäläinen 2002). It includes models for reflooding and radiation heat transfer from fuel rod to the subchannel. GENFLO solves the coolant mass, momentum and energy conservation equations. It also computes the axial distributions of the fluid temperature and the fluid void fraction. The resulting fluid temperatures and heat transfer coefficients at each axial level for each time step are supplied to FRAPTRAN, which calculates temperatures and deformation of the fuel pellets and cladding, including possible ballooning, see figure 4. The fuel specific computations are made by FRAPTRAN and the coolant specific calculations by GENFLO, for both codes. In the coupled code, FRAPTRAN is the main program calling GENFLO, which offers the thermal-hydraulic conditions for the entire subchannel. This computation is made only once for each time step, even if a number of iterations is done in FRAPTRAN during the time step. At the start, GENFLO is used to make a steady-state computation prior to any coupled code calculation. In the coupled code computation, FRAPTRAN dictates the time step length, typically 0.01-0.05 s, but the calculation is fast since GENFLO is non-iterative and effective numerical methods are applied (Daavittila, Hämäläinen, and Räty 2005). The FRAPTRAN-GENFLO code package has been used in the past for the pre- and post-test analyses of LOCA experiments performed at the Halden reactor (Miettinen, Stengård, and Kelppe 2004).

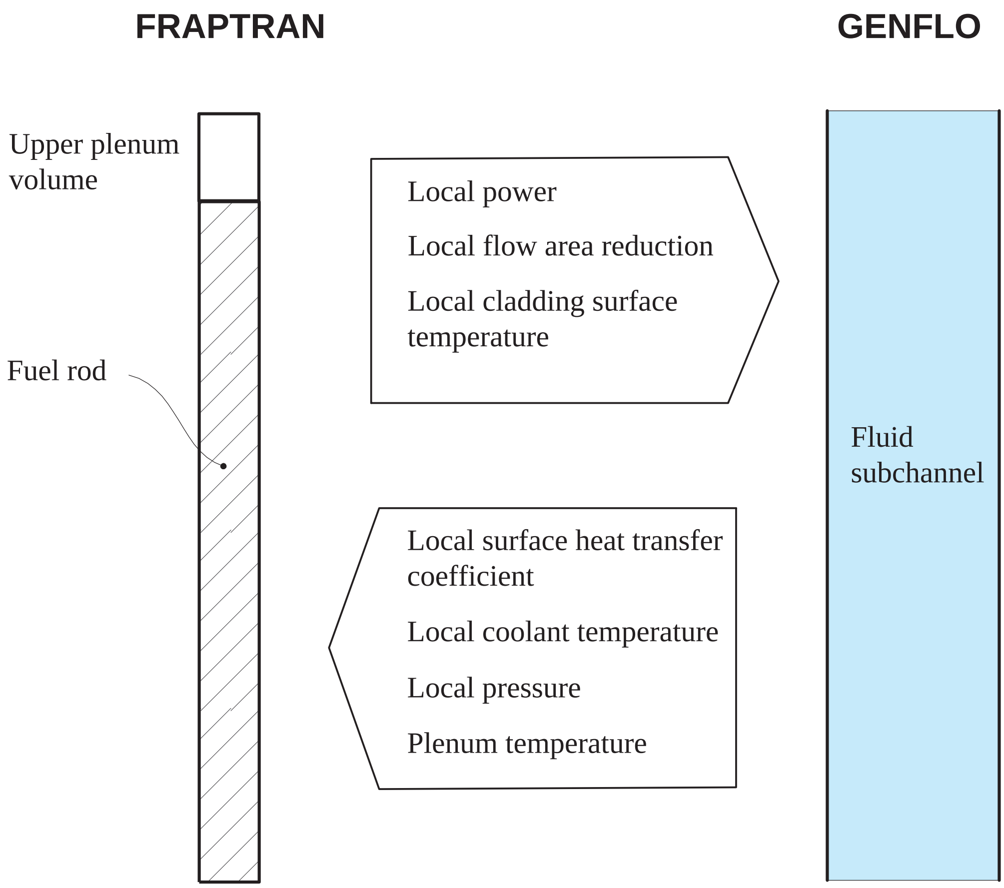

Figure 4: Coupling and data exchange in FRAPTRAN−GENFLO.

4 Calculations

Analyses of tests 5, 6 and 7 of the IFA-650 series using the FRAPTRAN code are presented in this section. The results from the calculations are compared with measured data for the following parameters:

- Cladding temperature as a function of time,
- Fuel rod pressure as a function of time,
- Cladding diameter at rupture versus axial position of rod,
- Peak cladding temperature at rupture and
- Maximum increase of outer surface oxide layer thickness of cladding tube induced by LOCA transient.

The transient fuel rod calculations of the IFA-650 tests presented in this work involve two versions of the FRAPTRAN code described in the foregoing section. The FRAPTRAN -QT1.4c calculations of the IFA-650 tests use thermal-hydraulic boundary conditions calculated by FRAPTRAN-GENFLO code (Miettinen, Stengård, and Kelppe 2004). More precisely, we apply the calculated time variations of coolant pressure, cladding outer surface temperatures as prescribed boundary conditions for the cladding in the calculations with the FRAPTRAN-QT1.4c code. Also the plenum temperature for the FRAPTRAN-QT1.4c code are derived from the FRAPTRAN-GENFLO calculations. For cladding failure, FRAP TRAN-GENFLO uses a strain-base cladding failure criterion, hoop strain versus burst temperature, whereas FRAPTRAN-QT1.4c, besides this option (not used here), employs stress-base failure criteria, hoop stress versus burst temperature (cf. Appendix A).

The active length of the test fuel rods is divided into 10 axial segments, each of equal length. The cladding is structurally treated as a thin-walled tube, i.e. it is represented by a single finite element across its thickness. The input options defining the cladding models selected in the FRAPTRAN calculations, presented in this section, are summarized in Appendix A. The input instructions for the FRAPTRAN-1.4 code are specified in (Geelhood, Luscher, and Beyer 2011b), whereas the additional input needed for use of the new cladding material models for LOCA analysis in FRAPTRAN-QT1.4c is described in (Jernkvist 2012). The time equal to zero (t=0) in the analyses refers to the start of blowdown. A constant time step length of 5 ms is used in the heat-up phase of the LOCA transient.

The present GENFLO model for heat transfer and calculation of coolant conditions is not perfectly suitable for test rig and coolant arrangements like that of IFA-650. For tests without particle filter (e.g. test 7, dealt with in this report, and tests 2, 3 and 4 reported in (Manngård, Massih, and Stengård 2012)) the temperature rise in the cladding after the blowdown is calculated to start approximately at the right time and also the subsequent temperature rise rate is in reasonable agreement with measurement. The agreement between the cladding temperatures calculated by GENFLO and the measurements is in general better at rod's lower end than at its upper end. Thus, GENFLO tends to overestimate the temperatures in the upper part of the rod. Tests with the particle filter installed (tests 5 and 6) are more challenging for GENFLO to simulate compared to tests without filter. The delay in cladding temperature rise (during heat-up) in the measured lower and upper thermocouple signals, predominantly in tests 5 and 6 using particle filter, cannot be properly modelled in the present version of the GENFLO program. In order to capture the measured delay of temperature rise after the blowdown (in tests 5 and 6) an increase of the tube wall friction for the water flow in the blowdown line and spray line was introduced. The delay of the temperature rise can in this way be extended in the GENFLO calculation, but the measured large differences between the cladding temperatures of the upper and lower end positions cannot be obtained. The increase of the tube wall friction may also result in a slower decrease of the coolant pressure calculated by GENFLO, which, in turn, may affect the overall calculation results.

4.1 Fuel rod initial state

The FRAPTRAN-GENFLO calculations of pre-irradiated test rods, used in the IFA-650 experiments 5, 6 and 7, are performed with burnup-dependent initial state calculated by the fuel rod steady-state behaviour code FRAPCON-3.4. Both calculations, by FRAPCON and FRAPTRAN, use 10 axial nodes to resolve fuel rod's active length. The nodal linear heat generation rates (LHGRs) for the FRAPCON-3.4 calculations are obtained from the fuel rod base irradiation power histories by assuming a slightly skewed axial power distribution with maximum at the upper end of the rod. Moreover, the finite element (FE) based mechanical cladding module of the codes (Knuutila 2006) is applied consistently in both the FRAPCON and FRAPTRAN calculations. Application of the FE analysis (FEA) model in FRAPCON produces an unformatted file for FRAPTRAN. Also, FRAPCON produces a formatted restart file for each time step, and the last time step information is used for FRAPTRAN. Because the rods are refabricated for the considered tests (from a full-length rod to a short test rod) a few modifications are made to the restart files. The amount of gas (mole) and its composition should correspond to the new rod filling. The new amount of gas is tuned by calculation of the first time step by FRAPTRAN at zero power and adjusted to get the correct initial pressure, i.e. the fill pressure of the refabricated rod.

Fuel rod irradiation (power) history primarily influences fission product gas release, i.e. the gas composition in the rod and thereby the rod internal gas pressure. These quantities were reset to predefined values in the considered IFA-650 LOCA tests 5, 6, and 7 (see table 1) upon re-fabrication after their respective pre-irradiation. Moreover, fuel deformation and restructuring, and cladding deformation are mainly burnup/exposure dependent, meaning that the details of power history have secondary effects on these quantities. Therefore, the effects of pre-irradiation simulations with FRAPCON on LOCA test simulations with FRAPTRAN should be slight.

The LOCA calculations of the IFA-650 tests by FRAPTRAN-QT1.4c are performed without FRAPCON-calculated initial fuel rod state, since verification calculations have shown that the impact of pre-irradiation on FRAPTRAN LOCA analysis results are small. Verification calculations were performed to check the influence of omitting the FRAPCON initialization (burnup-dependent rod state) on the final LOCA analysis results generated by the FRAPTRAN code. The differences between the two approaches, that is, LOCA analysis with and without FRAPCON initialization, were not significant. Thus LOCA analysis of a pre-irradiated test rod can be performed with sufficient accuracy by only using FRAPTRAN, i.e. by regarding the pre-irradiated rod as an unirradiated fuel rod, but with a reset gas gap composition and rod internal pressure, and also by altered rod dimensions.

4.2 Coolant conditions and plenum temperature

The coolant pressure, cladding outside temperature and plenum temperature as a function of time for the IFA-650 tests 5, 6 and 7 are calculated by using `FRAPTRAN-GENFLO`. The results are presented below.

Coolant pressure: The time variations of calculated coolant pressure in the IFA-650 tests 5, 6 and 7, using `FRAPTRAN-GENFLO`, are plotted in figure 5. The depressurising of pressure vessel (flask) in the blowdown phase (from roughly 7 MPa down to rig pressure ≈ 0.4 MPa) in the tests takes about 168, 165 and 114 s, respectively. The blowdown time considerably longer for the filter-equipped tests 5 and 6, than that for test 7, which had no filter. The transient LOCA calculations are carried out to 800 s after the initiation of the blowdown. The calculated coolant pressure boundary conditions by `FRAPTRAN-GENFLO` are prescribed in the succeeding calculations by the `FRAPTRAN-QT1.4c` code.

Cladding outer temperature: The time variations of cladding outer surface temperature in the IFA-650 tests 5, 6 and 7, using `FRAPTRAN-GENFLO`, are plotted in figures 6a, 6b and 7, respectively. The calculated cladding temperatures are given in the thermocouple positions (TCC) used in the various tests. The calculated temperatures are in reasonable agreement with the measured temperature recordings. The cladding temperature boundary conditions calculated by `FRAPTRAN-GENFLO` are prescribed in the calculations made by the `FRAPTRAN-QT1.4c` code.

Plenum gas temperature: The time variations of plenum gas temperature in the IFA-650 tests 5, 6 and 7, calculated by `FRAPTRAN-GENFLO`, are plotted as solid lines in figures 8, 9a and 9b, respectively. The plenum gas temperature variations shown by the dashed lines in these three figures represent simplified responses created from the calculated responses (solid lines) and are prescribed in the `FRAPTRAN-QT1.4c` calculations.

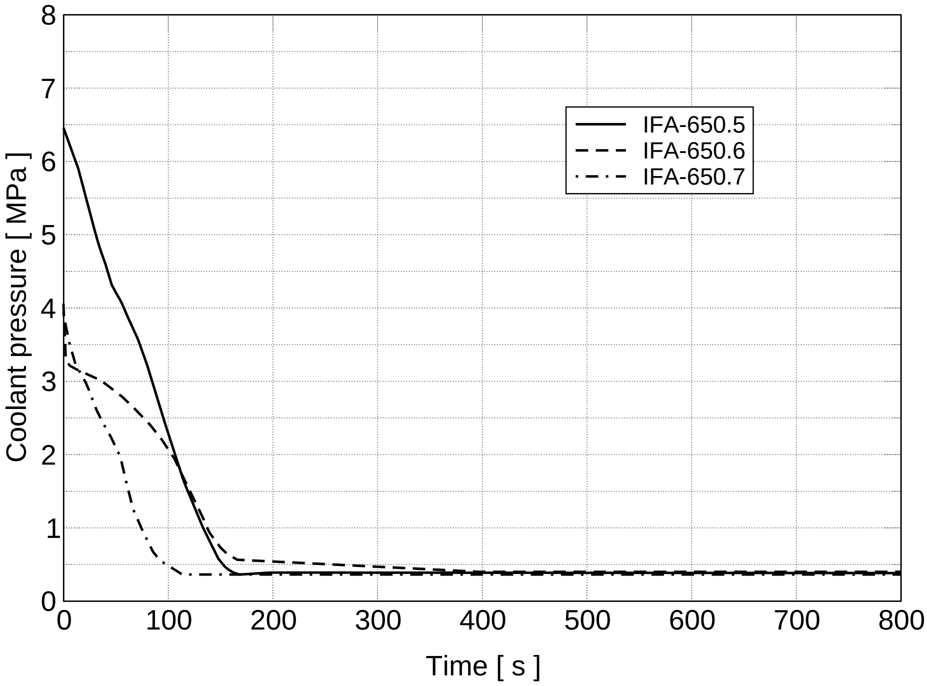

Figure 5: Calculated coolant pressure (rig pressure) variations with time for the IFA-650 tests 5, 6 and 7 using the `FRAPTRAN-GENFLO` code. The calculated coolant pressure boundary conditions by `FRAPTRAN-GENFLO` are prescribed in the calculations by the `FRAPTRAN-QT1.4c` code.

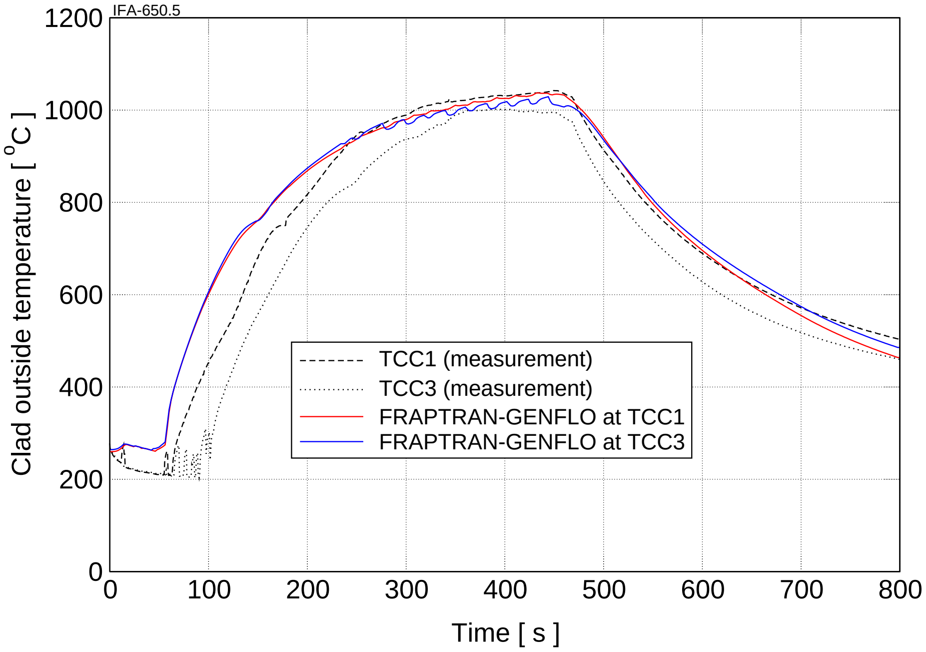

(a)

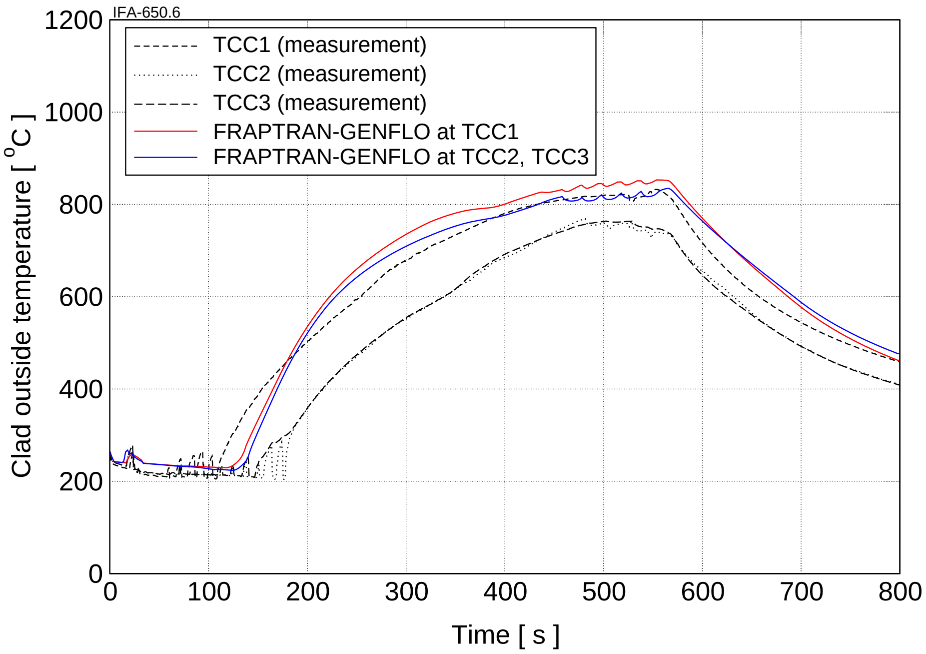

(b)

Figure 6: (a) IFA-650.5 (b) IFA-650.6 / Measured and calculated cladding outer surface temperatures in thermocouple positions. The axial positions of the cladding thermocouples (TCC) for the tests are given in table 2. The calculated cladding temperature boundary conditions by `FRAPTRAN-GENFLO` are prescribed in the calculations by the `FRAPTRAN-QT1.4c` code.

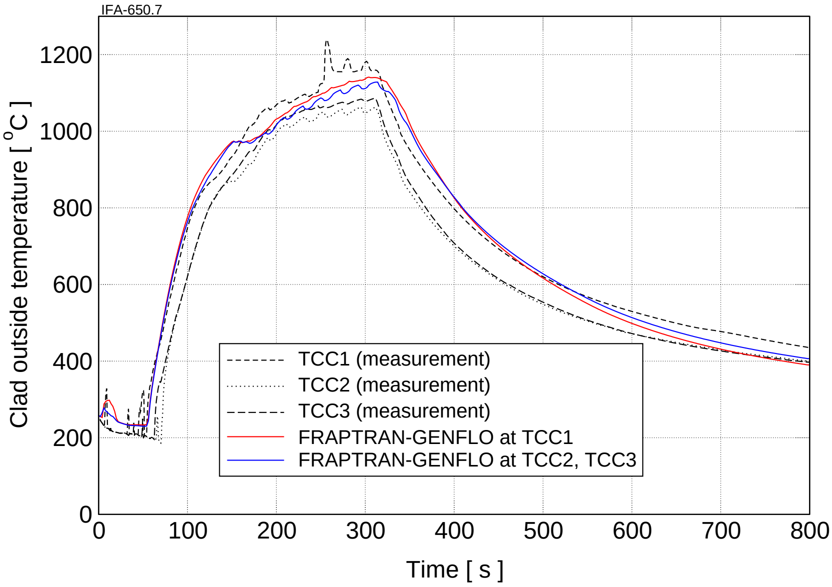

Figure 7: IFA-650.7 / Measured and calculated cladding outer surface temperatures in thermocouple positions. The axial positions of the cladding thermocouples (TCC) for the test are given in table 2. The calculated cladding temperature boundary conditions by `FRAPTRAN-GENFLO` are prescribed in the calculations by the `FRAPTRAN-QT1.4c` code.

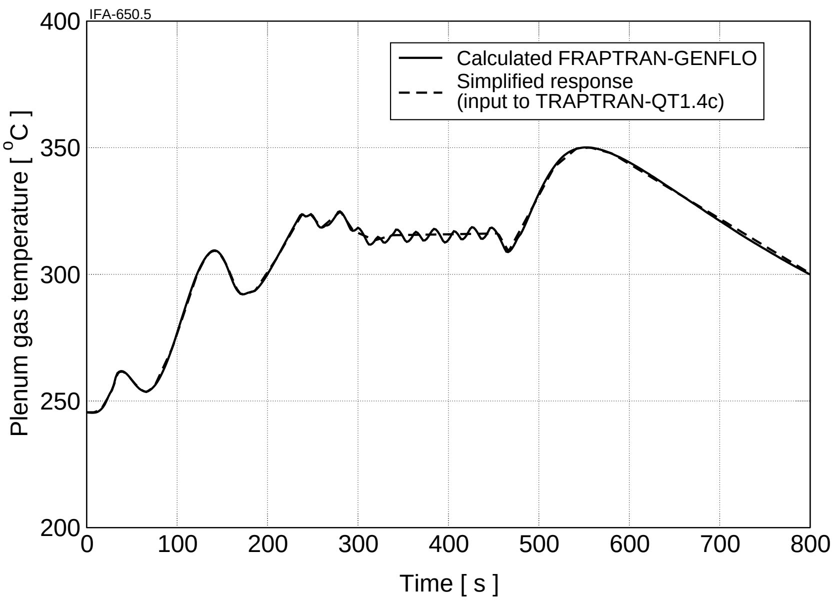

Figure 8: IFA-650.5 / Solid line; `FRAPTRAN-GENFLO` calculated time variation of plenum gas temperature. Dashed line; Simplified curve of the calculated response. The plenum gas temperature described by the dashed line is prescribed in the IFA-650.5 calculations by the `FRAPTRAN-QT1.4c` code.

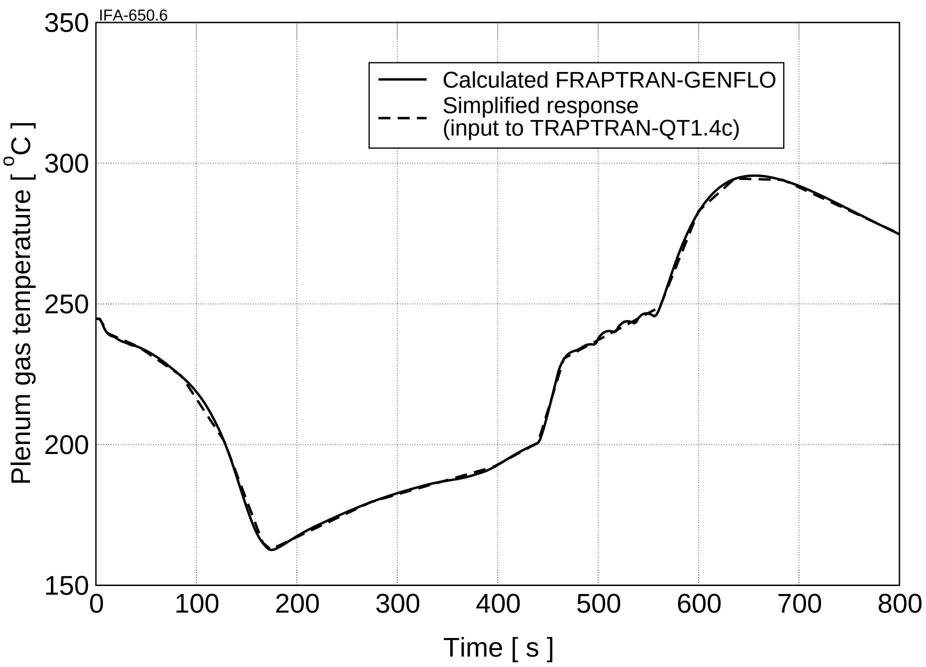

(a)

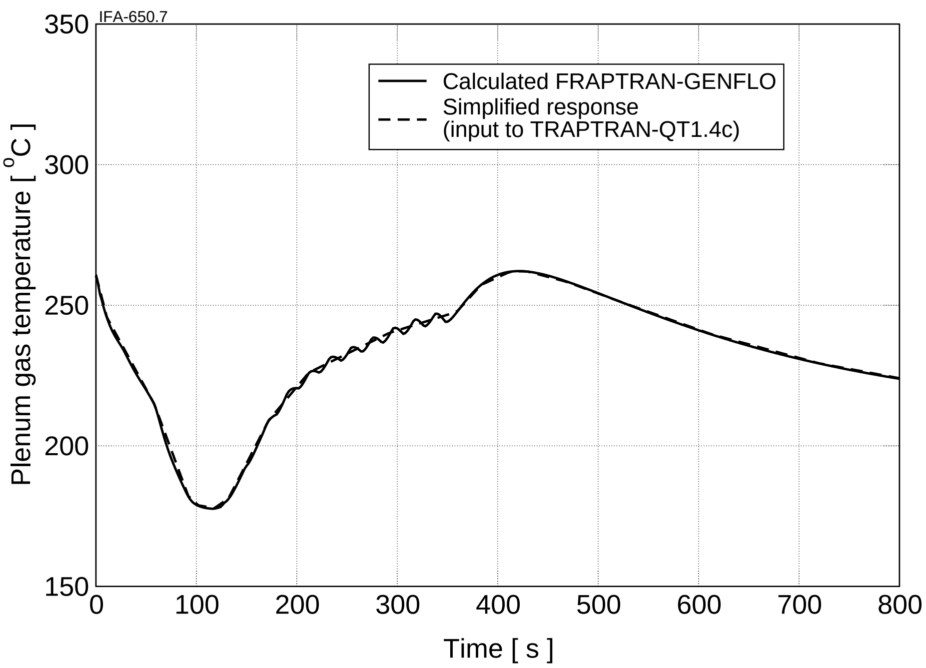

(b)

Figure 9: (a) IFA-650.6 (b) IFA-650.7 / Solid line; `FRAPTRAN-GENFLO` calculated time variation of plenum gas temperature. Dashed line; Simplified curve of the calculated response. The plenum gas temperature described by the dashed line is prescribed in the IFA-650.6/7 calculations by the `FRAPTRAN-QT1.4c` code, respectively.

4.3 Rod gas pressure

The rod gas pressure (plenum pressure) as a function of time for the IFA-650 tests 5, 6 and 7, calculated by `FRAPTRAN-GENFLO` and `FRAPTRAN-QT1.4c`, are compared with measurements in figures 10, 11 and 12, respectively. The rod gas pressure in these figures, calculated by `FRAPTRAN-GENFLO`, are shown as solid lines, whereas the `FRAPTRAN-QT1.4c` results are shown as dashed lines. The measured time responses of the rod pressure (PF signal) are plotted as dash-dot lines.

4.3.1 IFA-650.5

The cladding rupture in the experiment occurred 178 s after the start of the blowdown at a cladding temperature around 750°C. Shortly after this moment the measured rod pressure showed a distinct drop (from $\approx$ 7.2 MPa) followed by a gradual decrease in the pressure over time. The equilibration of the rod gas pressure down to the rig pressure after cladding rupture took about 2 minutes (120 s), see figure 10 (Kekkonen 2007a). The occurrence of cladding rupture obtained in the experiment is indicated by an asterisk in this figure. The calculated times to cladding rupture by the `FRAPTRAN-GENFLO` and `FRAPTRAN-QT1.4c` codes are 198 and 157 s, respectively. These rupture points are indicated by the cross symbol ($\times$) in figure 10. The calculated rod pressures at these instants, but just before cladding rupture, are 4.6 and 5.9 MPa, respectively.

4.3.2 IFA-650.6

The cladding rupture obtained in the experiment occurred 525 s after the start of the blowdown. The cladding temperature at rupture was measured to be about 830°C. The measured rod pressure, just prior to cladding rupture in the experiment, was 6.4 MPa. It should be noted that the absolute rod pressure level in the pressure measurement could not be defined precisely for the test (Kekkonen 2007b). However, upon cladding failure the rod pressure dropped rapidly down to the rig pressure. The measured pressure signal is shown by the dash-dot line in figure 11 (Kekkonen 2007b). The times to cladding rupture calculated by the `FRAPTRAN-GENFLO` and `FRAPTRAN-QT1.4c` codes are 530 and 455 s, respectively (figure 11). The calculated rod pressures shortly before rupture are 4.2 and 4.1 MPa, respectively. In figure 11, we have also plotted a response of the rod pressure, calculated by `FRAPTRAN-QT1.4c`, in which the prescribed cladding outer surface temperatures were reduced by 3% relative to the original (`GENFLO`-calculated) temperature boundary condition. The rod pressure evolution of this additional calculation is shown by the curve plotted with the short dashes in figure 11. The cladding rupture calculated for this case occurs 518 s after the start of the blowdown.

4.3.3 IFA-650.7

The fuel rod cladding in the experiment failed 247 s after the start of the blowdown at a cladding temperature around 1100°C. At this rupture temperature (1100°C) practically all of the cladding material (in failure location) undergoes phase transformation from α-phase to β-phase. The measured rod pressure shortly before cladding rupture was 1.05 MPa. After failure the rod pressure fell rapidly down to the rig pressure. The times to cladding rupture calculated by `FRAPTRAN-GENFLO` and `FRAPTRAN-QT1.4c` are 194 and 213 s, respectively (figure 12). At these time instants (prior to rupture) the calculated rod pressures are 0.89 and 0.86 MPa, respectively.

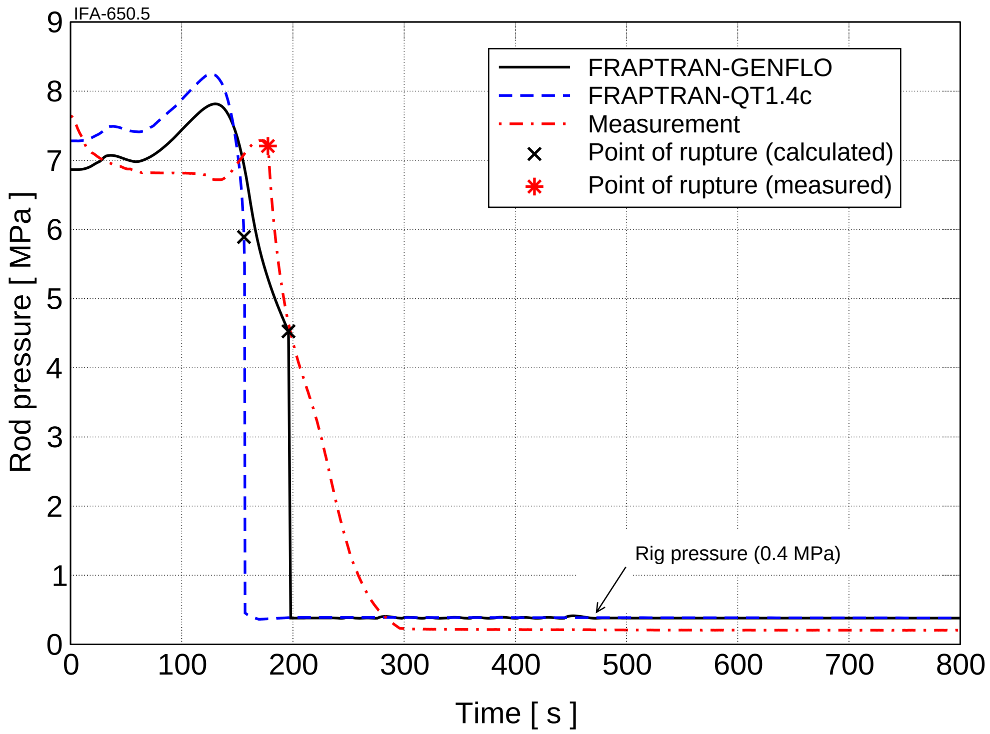

Figure 10: Rod gas pressure (plenum pressure) vs. time for the IFA-650.5 test calculated by the `FRAPTRAN-GENFLO` (solid line) and `FRAPTRAN-QT1.4c` (dashed line) codes. Cladding rupture is calculated at 198 and 157 s after start of blowdown, respectively. The measured evolution of the rod pressure is shown by the dash-dot curve. The calculated points of rupture are marked with a star symbol ($\times$) and measured rupture point with an asterisk symbol.

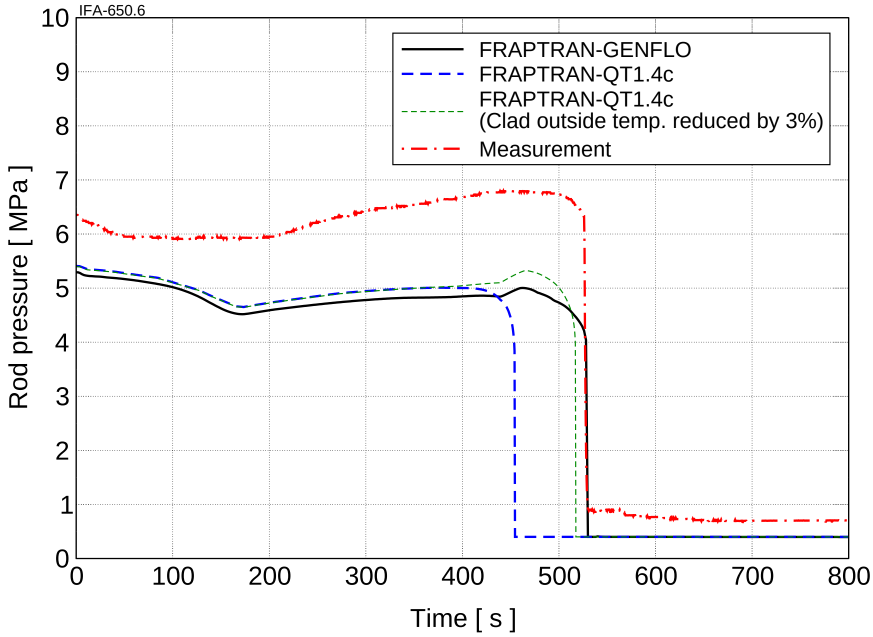

Figure 11: IFA-650.6 rod gas pressure variation with time calculated by the FRAPTRAN-GENFLO and FRAPTRAN-QT1.4c codes. The measured rod gas pressure variation during the transient is shown by the dash-dot curve (Kekkonen 2007b).

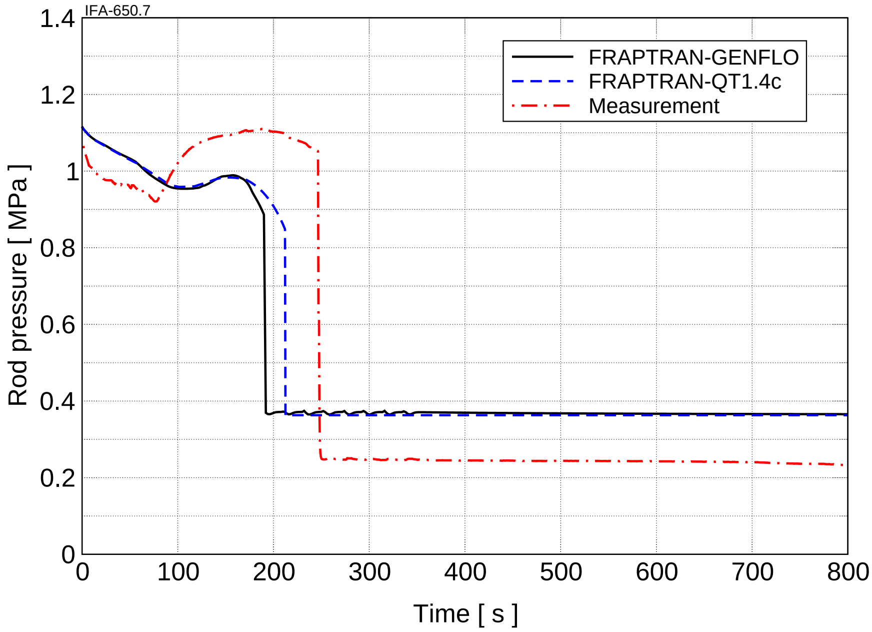

Figure 12: IFA-650.7 rod gas pressure variation with time calculated by the FRAPTRAN-GENFLO and FRAPTRAN-QT1.4c code. The measured rod gas pressure variation during the transient is shown by the dash-dot curve (Jošek 2008).

4.4 Cladding deformation and rupture

4.4.1 IFA-650.5

The calculated and measured cladding outer diameter profiles over the fuel stack region at burst are compared in figure 13. The two profiles plotted as solid and dashed lines are the results from calculations using the FRAPTRAN-GENFLO and FRAPTRAN-QT1.4c codes, respectively. The measured post-test cladding diameter profile for the IFA-650.5 rod, obtained by visual inspection (VI) and by neutron radiography (NR) (Oberländer, Espeland, and Jenssen 2008), are given as dash-dot lines in figure 13. The maximum measured diameter value (≈ 12.5 mm) from VI in cladding's failure position is shown by an asterisk symbol and is located about 70 mm from the fuel stack lower end. The corresponding maximum diameter from NR measurement is ≈ 14 mm. The initial cladding diameter of the test rod was 10.735 mm. The letter symbol "T" in figure 13 indicates axial location of cladding thermocouples (table 2).

The calculated diameter profile at rupture by FRAPTRAN-QT1.4c is sharper than that obtained by the FRAPTRAN-GENFLO code. Cladding rupture, by both codes, is calculated in axial node 5, i.e. in the rod's peak power position. This axial node corresponds to an axial elevation of 0.216 m from bottom end of the fuel stack, cf. figure 13. The maximum cladding diameters calculated by the FRAPTRAN-GENFLO and FRAPTRAN-QT1.4c codes, are 15.8 and 19.7 mm, respectively, and are marked by ring symbols (figure 13). The axial elevation of the failure position in the calculations is governed by the cladding outer surface temperatures (distribution along the rod) calculated by the thermal-hydraulics module GENFLO.

The measured cladding outer surface temperatures by the lower and upper end thermocouples (TCC1 and TCC3, respectively, see figure 6a) show typically a difference of 100-150°C during the heat-up phase, whereas the corresponding difference between the cladding temperatures generated by GENFLO is very small. See also introductory comments on GENFLO calculations given in section 4. However, we should remember that neither the actual magnitude of cladding temperature at mid (peak power) position nor its axial distribution is known from the test. The cladding temperature was measured by thermocouples located at rod's lower and upper ends. The measured cladding deformation profiles suggest that the rod may have experienced higher temperatures at its lower end than in the mid and upper locations. Thus, in future tests, it would be desirable to measure the cladding temperature by a thermocouple located at rod's mid position.

4.4.2 IFA-650.6

The calculated and measured cladding outer diameter profiles over the fuel stack region at burst for the IFA-650.6 test rod are compared in figure 14. The two profiles plotted by the solid and dashed lines are the results from calculations using the FRAPTRAN-GENFLO and FRAPTRAN-QT1.4c codes, respectively. The measured post-test cladding diameter profile for the IFA-650.6 rod is given as dash-dot line in figure 14. The maximum measured diameter value (≈ 13.2 mm) in cladding's failure position is shown by an asterisk symbol and is located about 90 mm from the fuel stack lower end, i.e. just below the lower thermocouple position. Axial level of cladding thermocouple positions is indicated by letter symbol "T" in figure 14. The initial cladding diameter of the test rod was 9.13 mm.

The calculated cladding deformations at rupture by FRAPTRAN-GENFLO and FRAPTRAN-QT1.4c are in close agreement. Cladding rupture, by both codes, is calculated in axial node 4. This axial node corresponds to an axial elevation of 0.168 m from bottom end of the fuel stack, figure 14. The maximum cladding diameters calculated by the FRAPTRAN-GENFLO and FRAPTRAN-QT1.4c codes, amount to 15.7 and 17.3 mm, respectively. Similarly as in the previous test (IFA-650.5), the measured cladding outer surface temperatures by the lower and upper end thermocouples (TCC1 and TCC2/TCC3, respectively, see figure 6b) show typically a difference of 100-150°C during the heat-up phase, whereas the corresponding difference in the cladding temperatures generated by GENFLO is very small. See also introductory comments on GENFLO calculations given in section 4. The discussion regarding cladding temperature measurement in the test given for IFA-650.5 is also valid for IFA-650.6 test, that is, that neither the actual magnitude of cladding temperature at mid (peak power) position nor its axial distribution is known from the test. The cladding temperature is measured by thermocouples, located at rod's lower end and at its upper end. The measured cladding deformation profile suggests that the rod may have experienced higher temperatures at its lower end than in the mid and upper locations. Moreover, since the cladding rupture occurred very close to the lower thermocouple, it cannot be fully ruled out that its attachment to the cladding may have made the location more prone to deformation and failure than rod's peak power position.

4.4.3 IFA-650.7

The calculated and measured cladding outer diameter profiles over the fuel stack region at burst for the IFA-650.7 test rod are compared in figure 15. The two profiles plotted by the solid and dashed lines are the results from calculations using the FRAPTRAN-GENFLO and FRAPTRAN-QT1.4c codes, respectively. The measured post-test cladding diameter profile for the IFA-650.7 rod is given as dash-dot line in figure 15. The measured cladding diameter profile at burst plotted in figure 15 is the average of two orientations obtained at 0° and 45° (Oberländer and Jenssen 2011b). The cladding diameter increase is significant and fairly uniform (14-22%) over almost entire length of the rod. No evident signs of local ballooning is seen in the measured diameter profile. The maximum measured diameter value ($\approx$ 11.7 mm) in cladding's failure position is shown by an asterisk symbol and is located roughly 125 mm from the fuel stack lower end. The initial cladding diameter of the test rod was 9.62 mm. The letter symbol "T" in the figure indicates cladding thermocouple position.

The differences in cladding deformations calculated by FRAPTRAN-GENFLO and FRAPTRAN-QT1.4c for the IFA-650.7 test are small. Cladding rupture, by both codes, is calculated in axial node 5, i.e. in the rod's peak power position. This axial node corresponds to an axial elevation of 0.216 m from bottom end of the fuel stack, cf. figure 15. The maximum cladding diameters calculated by the FRAPTRAN-GENFLO and FRAPTRAN-QT1.4c codes, are 12.4 and 12.5 mm, respectively, and are marked by ring symbols (figure 15).

The evaluation of the IFA-650 tests 5, 6 and 7 performed in this report is summarized in table 4. The calculated cladding rupture times for these tests in the FRAPTRAN-1.4 program documentation (Geelhood, Luscher, and Beyer 2011c) are 169, 423 and 152 s, respectively. We should point out that Geelhood and company (Geelhood, Luscher, and Beyer

2011c) applied the FRACAS-1 analytical thin-shell cladding model in their calculations, whereas in present calculations we apply the optional finite element based cladding model (FEA) available in the code.

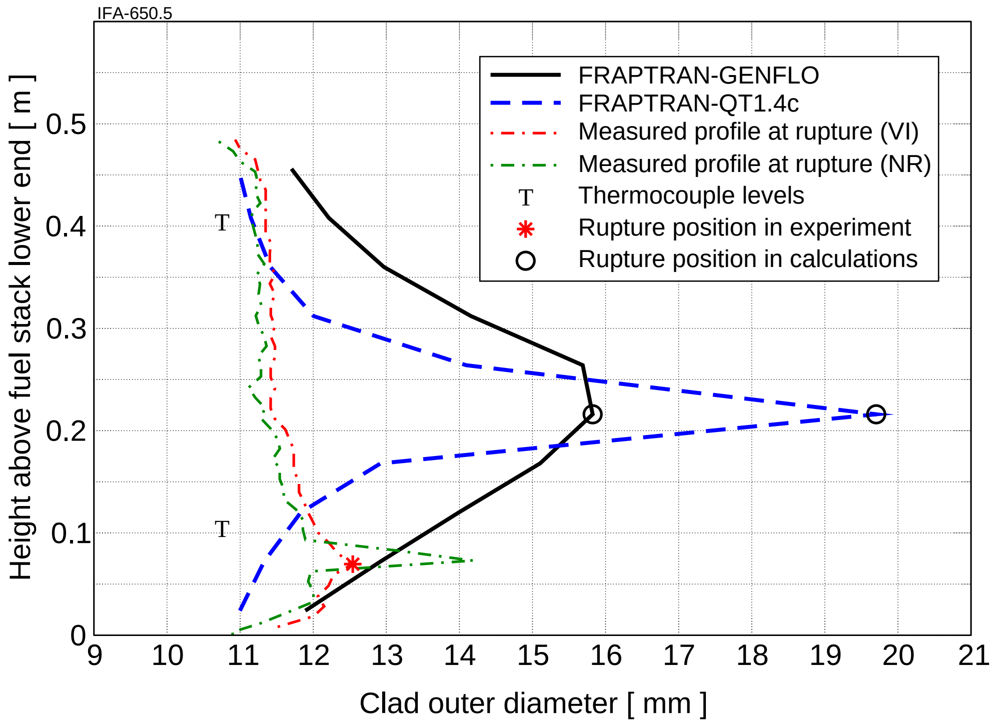

Figure 13: IFA-650.5 rod calculated and measured outer diameter profiles of cladding at burst. The two profiles shown by the solid and dashed lines represent the calculations made by FRAPTRAN-GENFLO and FRAPTRAN-QT1.4c, respectively. The corresponding measured diameter profiles obtained by visual inspection (VI) and neutron radiography (NR) are shown by the dash-dot lines (Oberländer, Espeland, and Jenssen 2008) and maximum measured diameter from VI is marked by asterisk.

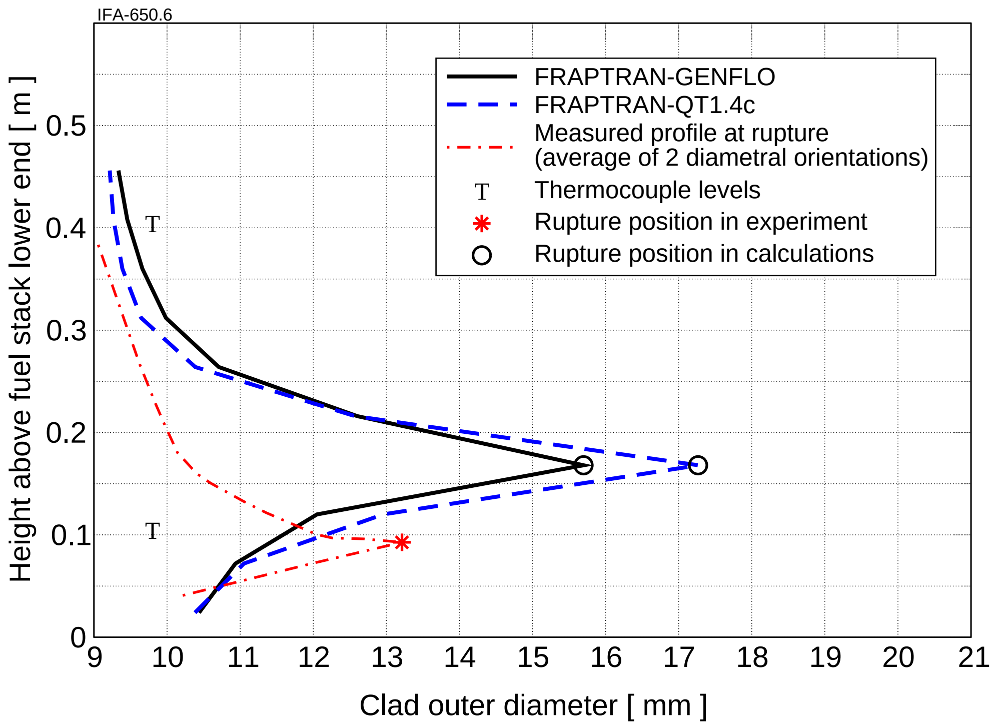

Figure 14: IFA-650.6 rod calculated and measured outer diameter profiles of cladding at burst. The two profiles shown by the solid and dashed lines represent the calculations made by `FRAPTRAN-GENFLO` and `FRAPTRAN-QT1.4c`, respectively. The corresponding measured diameter profile is shown by the dash-dot line (Kekkonen 2007b) and maximum measured diameter by asterisk.

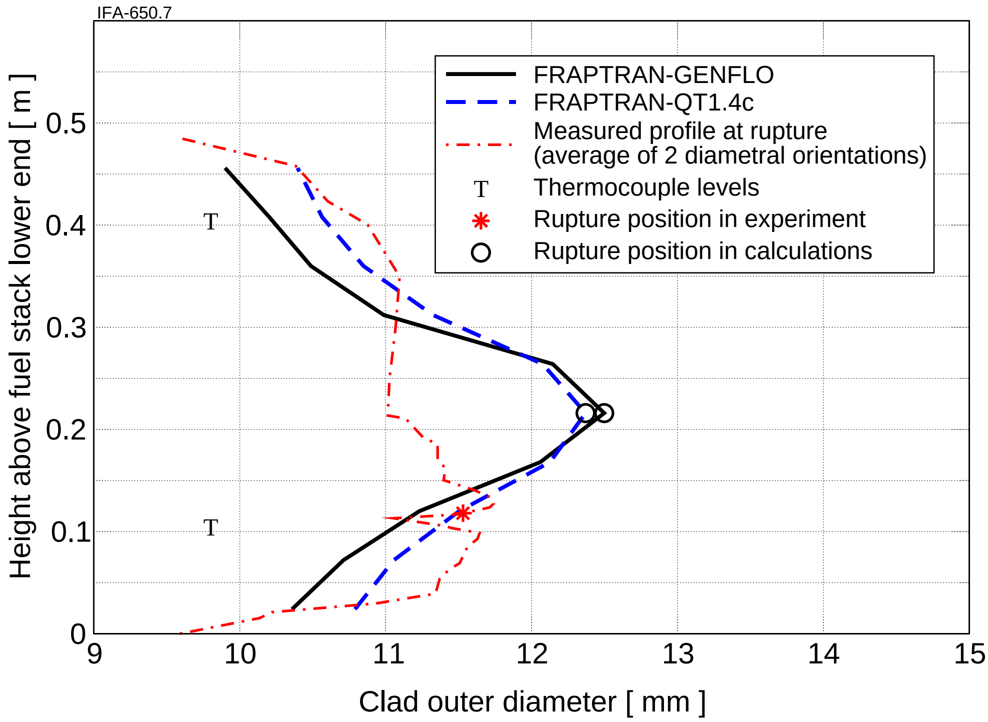

Figure 15: IFA-650.7 rod calculated and measured outer diameter profiles of cladding at burst. The two profiles shown by the solid and dashed lines, respectively, represent the calculation outcome by the `FRAPTRAN-GENFLO` and `FRAPTRAN-QT1.4c` codes. The measured diameter along the rod is shown by the dash-dot line (Oberländer, Espeland, Solum, and Jenssen 2008) and maximum measured diameter by asterisk.

Table 4: Comparison of calculated and measured results for the IFA-650 tests 5, 6 and 7.

Test/ Parameter	Calculation 1)	2)	Measurement
IFA-650.5/			
Time to cladding rupture, s	198	157	178
Rupture temperature, °C	896	801	750
Max. diametral cladding strain, %	47$^\flat$	84$^\flat$	16
Rod pressure at rupture, MPa	4.6	5.9	7.2
Outer surface oxide layer, μm (increase under LOCA)	8	5	11
IFA-650.6/			
Time to cladding rupture, s	530	455/518†	525
Rupture temperature, °C	853	840/822†	830
Max. diametral cladding strain, %	72$^\flat$	89$^\flat$/90$^{\flat\dagger}$	36
Rod pressure at rupture, MPa	4.2	4.1/4.2†	(6.4)‡
Outer surface oxide layer, μm (increase under LOCA)	1.5	3.5/2.5†	2
IFA-650.7/			
Time to cladding rupture, s	194	213	247
Rupture temperature, °C	1056	1092	1100
Max. diametral cladding strain, %	30$^\flat$	29$^\flat$	24
Rod pressure at rupture, MPa	0.89	0.86	1.05
Outer surface oxide layer, μm (increase under LOCA)	23	29	30

1) `FRAPTRAN-GENFLO`

2) `FRAPTRAN-QT1.4c`

$^\flat$ Value obtained from the calculated increase of cladding outer diameter relative to initial cladding diameter of test fuel rod.

† Results (after the / symbol) are obtained by applying a 3% reduction on the prescribed cladding outside surface temperatures (from heat-up until end of calculation).

‡ The level of absolute rod pressure could not be defined precisely in the IFA-650.6 test (Kekkonen 2007b).

5 Summary highlights

Here, we briefly summarize our evaluations of the Halden IFA-650 LOCA tests 2, 3 and 4, reported in (Manngård, Massih, and Stengård 2012), and the subsequent tests 5, 6 and 7, dealt with, in the present report. The tests are evaluated using two versions of the transient fuel rod code `FRAPTRAN-1.4`, namely `FRAPTRAN-GENFLO` and `FRAPTRAN-QT1.4b/c`. The sole difference between the subversions `QT1.4b` (used in (Manngård, Massih, and Stengård 2012)) and `QT1.4c` (used here) of the `FRAPTRAN` program is that the latter has been extended with material models for Zr1%Nb cladding needed for analysis of test 6. Since the `FRAPTRAN-GENFLO` code is coupled to a thermal-hydraulic program (`GENFLO`), that capability is also utilized to prescribe the fuel rod boundary conditions for the `FRAPTRAN-QT1.4b/c` analyses reported here. For cladding mechanical calculations, the finite element method option of the codes is invoked. The fuel rod initial conditions after base irradiation for FRAPTRAN-GENFLO were precalculated using the steady-state fuel performance code FRAPCON-3.4. Since, however, our computations showed that the impact of preirradiation on FRAPTRAN LOCA analysis results is small, the FRAPTRAN-QT1.4b/c calculations were done without FRAPCON initialization.

The fuel rod samples used in the considered tests (2, 3, 4, 5, 6 and 7) represent a variety of fuel rod designs and irradiation conditions. More specifically, test 2 used an unirradiated fuel rod sample with PWR characteristics, while tests 3 and 4 used irradiated PWR fuel rod samples with burnups of about 82 and 92 MWd/kgU, respectively. The fuel rod samples used in the tests 5, 6, and 7 represent three different designs, namely, PWR, VVER (Russian type of PWR) and BWR, respectively. The rod burnup of these respective test samples were about 83, 56 and 44 MWd/kgU. The PWR and VVER rods (tests 2, 3, 4, 5 and 6) failed during the LOCA tests at temperatures below and around 800°C by fuel cladding burst. The BWR rod (test 7) failed by cladding burst at 1100°C. The burst temperatures obtained in the experiments are much lower than the value (1204°C) set by the acceptance criteria. We note further that the maximum cladding deformation (diameter increase) in the tests 2, 3 and 4 develops near rod's mid-axial elevation, whereas that in the tests 5, 6 and 7 develops at rod's lower end.

Computations made by both FRAPTRAN-GENFLO and FRAPTRAN-QT1.4b/c produce cladding failure at about mid-axial elevation for all the six aforementioned tests, whereas the failures in the experiments occur either near mid-axial level or at lower end of the rods. The axial elevation of the failure position in the calculations is governed by the cladding outer surface temperatures (distribution along the rod) calculated by the thermal-hydraulics module GENFLO. The calculated rupture strains (cladding diameter increase at rupture) by both FRAPTRAN-GENFLO and FRAPTRAN-QT1.4b/c for tests 2, 4 and 7 are fairly close to the values obtained in the measurements. The cladding in test 3 ruptured prematurely (at low strain, <10%) at lower thermocouple position. Moreover, the rupture strains for tests 5 and 6 are overestimated by both codes. These two specific tests were equipped with an additional particle filter in the outlet flow line of the rig. For this situation (test configuration), the cladding temperature and its increase rate during heat-up is overestimated by the present version of GENFLO. The calculated rupture times and rupture temperatures for the tests 2, 3, 4 and 6 agree well with the measurements. For the tests 5 and 7 the agreement between calculations and measurements, regarding rupture time and temperature, is not as good as for the tests 2, 3, 4 and 6. Also, the differences between the burst results by the two codes for test 5 and 7 are somewhat larger than for the other tests.

One point worthwhile to note is that in our FRAPTRAN-QT1.4b calculations of the tests 2, 3 and 4, reported in (Manngård, Massih, and Stengård 2012), we used total oxygen concentration value (sum of oxygen content in metal and oxide layer) in the burst stress correlation, whereas in the actual FRAPTRAN-QT1.4c calculations (tests 5, 6 and 7) we instead apply the oxygen content in the metal to obtain the burst stress. To quantify the impact of the oxygen parameter on the cladding diameter increase at rupture in the tests 2, 3 and 4, these were rerun by the FRAPTRAN-QT1.4c code. These calculations showed that the change in the oxygen parameter increases the diameter at rupture by 0.2-0.6 mm, relative to the results in (Manngård, Massih, and Stengård 2012).

Finally, we should note that neither the actual magnitude of cladding temperature at mid (peak power) position nor its axial distribution is known from the tests. The cladding temperature was measured by thermocouples located at rod's lower and upper ends. The measured post-test cladding diameter profiles for tests 5, 6 and 7 suggest that the rods may have experienced higher temperatures at their lower ends than in the mid and upper locations. Thus, in future tests in the IFA-650 series, it would be desirable (if possible) to measure the cladding temperature by a thermocouple located at rod's mid position.

Acknowledgements

The work of T.M. was supported by the Swedish Radiation Safety Authority (SSM) under the contract number SSM2012/510, 2030048-08. The VTT part of the work has been funded from the Finnish Research Program on Nuclear Power Plant Safety SAFIR2014. We thank Anna Alvestav (SSM) for her helpful comments.

References

Daavittila, A., A. Hämäläinen, and H. Räty (2005). Transient and fuel performance analysis with VTT's coupled code system. In *Mathematics and Computation, Supercomputing, Reactor Physics and Nuclear and Biological Applications*, Palais des Papes, Avignon, France, September 12-15, 2005. American Nuclear Society.

Erbacher, F. J., H. J. Neitzel, H. Rosinger, H. Schmidt, and K. Wiehr (1982). Burst criterion of Zircaloy fuel claddings in a loss-of-coolant accident. In D. G. Franklin (Ed.), *Zirconium in the Nuclear Industry: Fifth Conference*, Volume ASTM STP 754, Philadelphia, USA, pp. 271–283. American Society for Testing and Materials.

Erbacher, F. J., H. J. Neitzel, and K. Wiehr (1990). Cladding deformation and emergency core cooling of pressurized water reactor in a LOCA: Summary description of the REBEKA program. Technical Report KfK 4781, Kernforschungszentrum Karlsruhe, Karlsruhe, Germany.

Forgeron, T., J. C. Brachet, F. Barcelo, A. Castaing, J. Hivroz, J. P. Mardon, and C. Bernaudat (2000). Experiment and modeling of advanced fuel rod cladding behavior under LOCA conditions: Alpha-beta phase transformation kinetics and EDGAR methodology. In G. P. Sabol and G. D. Moan (Eds.), *Zirconium in the Nuclear Industry: Twelfth International Symposium*, Volume ASTM STP 1354, West Conshohocken, PA, USA, pp. 256–278. American Society for Testing and Materials.

Geelhood, K. J., W. G. Luscher, and C. E. Beyer (2011a). FRAPCON-3.4: A computer code for the calculation of steady-state thermal-mechanical behavior of oxide fuel rods for high burnup. Technical Report NUREG/CR-7022, Vol. 1, US Nuclear Regulatory Commission.

Geelhood, K. J., W. G. Luscher, and C. E. Beyer (2011b). FRAPTRAN 1.4: A computer code for transient analysis of oxide fuel rods. Technical Report NUREG/CR-7023, Vol. 1, US Nuclear Regulatory Commission.

Geelhood, K. J., W. G. Luscher, and C. E. Beyer (2011c). FRAPTRAN 1.4: Integral assessment. Technical Report NUREG/CR-7023, Vol. 2, US Nuclear Regulatory Commission.

Jernkvist, L. O. (2012). Implementation of models for cladding high temperature metal-water reactions, phase transformation, creep and failure in the FRAPTRAN-1.4 computer program. Technical Report TR10-005, Quantum Technologies AB, Uppsala, Sweden.

Jošek, R. (2008). LOCA testing at Halden, The BWR experiment IFA-650.7. Technical Report HWR-906, Institutt for energiteknikk, OECD Halden reactor project, Halden, Norway.

Kaddour, D., S. Frechinet, A. F. Gourgues, J. C. Brachet, L. Portier, and A. Pineau (2004). Experimental determination of creep properties of zirconium alloys together with phase transformation. *Scripta Mater. 51*, 515–519.

Kekkonen, L. (2007a). LOCA testing at Halden, The PWR experiment IFA-650.5. Technical Report HWR-839, Institutt for energiteknikk, OECD Halden reactor project, Halden, Norway.

Kekkonen, L. (2007b). LOCA testing at Halden, The VVER experiment IFA-650.6. Technical Report HWR-870, Institutt for energiteknikk, OECD Halden reactor project, Halden, Norway.

Knuutila, A. (2006). Improvements on FRAPCON3/FRAPTRAN mechanical modelling. Technical Report VTT-R-11337-06, VTT Technical Research Centre of Finland, Espoo, Finland.

Manngård, T., L. O. Jernkvist, and A. R. Massih (2011). Evaluation of loss-of-coolant accident simulation tests with the fuel rod analysis code FRAPTRAN-1.4. Technical Report TR11-008, Quantum Technologies AB, Uppsala, Sweden.

Manngård, T., A. Massih, and J.-O. Stengård (2012). Evaluation of Halden IFA-650 loss-of-coolant accident experiments 2, 3 and 4. Technical Report TR11-006, Quantum Technologies AB, Uppsala, Sweden.

Manngård, T. and A. R. Massih (2010). Modelling of nuclear fuel cladding under loss-of-coolant accident conditions. Technical Report TR09-008, Quantum Technologies AB, Uppsala, Sweden.

Manngård, T. and A. R. Massih (2011). Modelling and simulation of reactor fuel cladding under loss-of-coolant conditions. *Journal of Nuclear Science and Technology 48*(1), 39–49.

Massih, A. R. (2008). A model for analysis of Zr alloy fuel cladding behaviour under LOCA conditions. Technical Report TR08-007, Quantum Technologies AB, Uppsala, Sweden.

Massih, A. R. (2009). Transformation kinetics of zirconium alloys under non-isothermal conditions. *J. Nucl. Mater. 384*, 330–335.

Van Uffelen, P., C. Győri, A. Schubert, J. van de Laar, Z. Hózer, and G. Spykman (2008). Extending the application range of a fuel performance code from normal operating to design basis accident conditions. *J. Nucl. Mater. 383*, 137–143.

Miettinen, J. and A. Hämäläinen (2002). GENFLO: A general thermal hydraulic solution for accident simulation. Technical Report 2163, VTT, Espoo, Finland.

Miettinen, J., J.-O. Stengård, and S. Kelppe (2004). FRAPTRAN-GENFLO Calculations on the IFA-650 LOCA Test. In *Proceedings of Enlarged Halden Programme Group Meeting 2004, May 9-14 (HPR-362)*, Volume 2, Sandefjord, Norway.

Oberländer, B. C., M. Espeland, and H. K. Jenssen (2008). LOCA testing of high burnup PWR fuel in the HBWR. Additional PIE on the cladding of the segment 650.5. Technical Report IFE/KR/E-2008/004, Institutt for energiteknikk, Kjeller/Halden, Norway.

Oberländer, B. C., M. Espeland, N. O. Solum, and H. K. Jenssen (2008). LOCA IFA650-4: PIE of the high burnup (92 MWd/kgU) PWR segment. In *Proceedings of Enlarged Halden Programme Group Meeting 2008, May 9-14 (HPR-362)*, Number SESSION: F2/PAPER:7, Loen, Norway.

Oberländer, B. C. and H. K. Jenssen (2011a). PIE results from a 56 MWd/kgU VVER segment after LOCA testing in IFA-650.6. Technical Report HWR-969, Institutt for energiteknikk, OECD Halden reactor project, Halden, Norway.

Oberländer, B. C. and H. K. Jenssen (2011b). PIE results from the low burnup ($\sim$44 MWd/kgU) BWR segment after LOCA testing in IFA-650.7. Technical Report HWR-925, Institutt for energiteknikk, OECD Halden reactor project, Halden, Norway.

Pihlatie, M. (2005). Loviisa VVER fuel tests in the Halden reactor: Main data from fuel pre-characterisation, reactor base irradiation and post-irradiation examinations. Technical Report HWR-824, Institutt for energiteknikk, OECD Halden reactor project, Halden, Norway.

Powers, D. A. and R. O. Meyer (1980, April). Cladding swelling and rupture models for LOCA analysis. Technical Report NUREG-0630, US NRC.

Rosinger, H. E. (1984). A model to predict the failure of Zircaloy-4 fuel sheathing during postulated LOCA conditions. *J. Nucl. Mater. 120*, 41–54.

Appendix A Input parameters for cladding models

The input parameters defining the cladding models and options applied in the FRAPTRAN calculations in section 4 of the report are described briefly in table A1, below. The default values are used for those options for which no values are given explicitly. The cladding model options are mainly set in the `$model` block of the FRAPTRAN input files. However, the `CladType` parameter is defined in the `$design` block of the input. Further details on the input instructions are given in (Geelhood, Luscher, and Beyer 2011b) and (Jernkvist 2012).

Table A1: Definition of FRAPTRAN cladding models and options used in the calculations of the IFA-650 tests.

Program	Cladding model/ & suboptions	Description of selections
FRAPTRAN-GENFLO	mechan=1/	FE cladding mechanical model (FEA)
	CladType=4 or 6	Type of cladding material: 4=Zircaloy-4 (default), 6=Zr1%Nb
	irupt=2	Apply strain criterion for heating rates ≤10°C/s from NUREG-0630, Powers and Meyer (1980) to determine cladding failure.
	ruptstrain	Maximum effective plastic+creep strain value (default=1.0)
	frcoef	Coulomb coefficient of friction in pellet/ cladding interface. (default=0.015)
	irefine=2	No mesh refinement in case of ballooning.
FRAPTRAN-QT1.4c	mechan=1/	See above
	CladType=4 or 6	See above
	icplcr=2	Calculate only high-temperature creep deformation in cladding.
	icmod=1 or 3	High-temperature cladding creep model option: 1=Zircaloy-4 Rosinger (1984), 3=Zr1%Nb (M5) Kaddour et al. (2004).
	iccrp=1	Calculate mixed-phase creep rate by interpolation between single-phase creep rates.
	irupt=5 or 8	Stress criterion to determine cladding failure: 5=Zircaloy-4 average correl. Rosinger (1984), 8=Zr1%Nb (E110) Van Uffelen et al. (2008).
	icrup=2	Use temperature + phase composition for calculating cladding mixed-phase burst stress
	plendef=0	No creep deformation of gas plenum walls.
	ruptstrain=3.0	Maximum effective plastic+creep strain value (default=1.0)
	frcoef	Coulomb coefficient of friction in pellet/ cladding interface. (default=0.015)
	irefine=2	No mesh refinement in case of ballooning.

Cladding models and options

FRAPTRAN-GENFLO: In the `FRAPTRAN-GENFLO` calculations with the `FEA` cladding module, the rupture criterion option `irupt=2` is used. This option selects the burst hoop strain versus burst temperature correlation for cladding heating rates $\leq$10°C/s (slow-ramp) defined in the NUREG-0630 document (Powers and Meyer 1980) as a rupture criterion. A similar burst correlation for $\geq$25°C/s (fast-ramp) is also defined in (Powers and Meyer 1980), which can be selected in `FRAPTRAN` by setting `irupt=1`. However, since the average heating rate during the heat-up phase in the considered IFA-650 tests is less than 10°C/s (table 3) we apply the former of these two burst options.

The `GENFLO` thermal-hydraulic code in the combined `FRAPTRAN-GENFLO` code is activated by specifying `genflo='on'` in the `$boundary` block of the `FRAPTRAN` input file. Besides the general thermal-hydraulic boundary conditions along the test rod, `GENFLO` also calculates the rod's plenum temperature, and by specifying the input parameter `PlenumTemp=2` (in `$model` block) this value can be used in thermal-mechanical part (`FRAPTRAN`) of the transient calculations by the `FRAPTRAN-GENFLO` code. We have used the `FEA` option for the mechanical analysis of the cladding (`mechan=1` in `FRAPTRAN`), where for the yield strength the NUREG/CR-6534 correlation in the `ckmn` subroutine of `FRAPTRAN` is employed. This correlation seems to provide slightly better results in the evaluations of the Halden LOCA tests than the standard yield strength correlation in `ckmn`. The standard `FRAPTRAN` options `PlenumTemp=0` or `1` cannot be used for this type of test rod and coolant flow. There is also a possibility to specify (prescribe) the plenum temperature as function of time (`PlenumTemp=3`) in VTT's `FRAPTRAN` version. This option was added to the `FRAPTRAN-QT1.4c` code for the analyses here.

FRAPTRAN-QT1.4c: In the `FRAPTRAN-QT1.4c` calculations of the IFA-650 tests, we use the aforementioned FE cladding module combined with certain high-temperature cladding material models introduced in the program (Jernkvist 2012). The extended capability of the code includes models for high-temperature oxidation, phase transformation, creep deformation and rupture. The integrated performance of selected material models for cladding rupture prediction under LOCA conditions has been verified against burst test data in Manngård and Massih (2010, 2011), whereas the performance of individual models is verified and tested in Massih (2008, 2009). In `FRAPTRAN-QT1.4c` besides the aforementioned strain-base cladding failure criterion there are stress-base failure criteria after the experimental works of Erbacher et al. (1982), Rosinger (1984), Forgeron et al. (2000) and Van Uffelen et al. (2008). We have applied Rosinger's average (best-estimate) stress-base failure criterion in our calculations for Zircaloy-4/-2 cladding and Van Uffelen et al.'s correlation for Zr1%Nb type of cladding. The plenum temperature for `FRAPTRAN-QT1.4c` calculations was extracted from `GENFLO` thermal-hydraulic calculations. The plenum temperature variation with time was prescribed using the option `PlenumTemp=3` (cf. also `FRAPTRAN-GENFLO` paragraph above).

The input options defining the cladding model options applied in the `FRAPTRAN` calculations are summarized in table A1.

2014:19

The Swedish Radiation Safety Authority has a comprehensive responsibility to ensure that society is safe from the effects of radiation. The Authority works to achieve radiation safety in a number of areas: nuclear power, medical care as well as commercial products and services. The Authority also works to achieve protection from natural radiation and to increase the level of radiation safety internationally.

The Swedish Radiation Safety Authority works proactively and preventively to protect people and the environment from the harmful effects of radiation, now and in the future. The Authority issues regulations and supervises compliance, while also supporting research, providing training and information, and issuing advice. Often, activities involving radiation require licences issued by the Authority. The Swedish Radiation Safety Authority maintains emergency preparedness around the clock with the aim of limiting the aftermath of radiation accidents and the unintentional spreading of radioactive substances. The Authority participates in international co-operation in order to promote radiation safety and finances projects aiming to raise the level of radiation safety in certain Eastern European countries.

The Authority reports to the Ministry of the Environment and has around 300 employees with competencies in the fields of engineering, natural and behavioural sciences, law, economics and communications. We have received quality, environmental and working environment certification.

Strålsäkerhetsmyndigheten
Swedish Radiation Safety Authority

SE-171 16 Stockholm
Solna strandväg 96

Tel: +46 8 799 40 00
Fax: +46 8 799 40 10

E-mail: registrator@ssm.se
Web: stralsakerhetsmyndigheten.se